

Bioencapsulation Innovations

November 2016

CONTENTS
EDITORIAL 1

XXIV Int. Conf. on Bioencapsulation

BRG GENERAL ASSEMBLY 2

ARTICLE - PONCELET AWARD

Stability and Gastro intestinal delivery of food bioactives

A. Brodkorb4

DIVERSIFIED INFOS 6

CALENDAR 7

ARTICLES - BEST STUDENT CONTRIBUTIONS

 Magnetic liposomes for remote controlled release of anticancer drug
 A. Petrunin8

 Encapsulation of endophytic *M. brunneum* for biological crop protection
 V. Krell 10

 Microchannel emulsification: a novel approach to cell encapsulation
 K.E. Markwick 12

 Custom-tailored sol-gel derived matrices for chemicals' immobilization
 M. Loureiro 14

 Oxygenation strategy to maintain encapsulated pancreatic islets in hypoxia
 A. Moure 16

 Innovative nanocarrier-based topical formulations for alopecia treatment ..
 L. Roque 18

 Enhancing thermal stability of vaccines using silica
 A. Doekhie 20

 Cell-selective encapsulation in hydrogel sheaths using antibody conjugated HRP
 M. Sengoku 22

 Production of carnauba wax particles for coating in fluidized bed
 B. Paulo 24

 Effect of free radicals produced by enzyme microcapsules on cancer cells
 M. Majerska 26

BIBLIOGRAPHY 28

ASSOCIATION 32

EDITORIAL
**XXIV INTERNATIONAL CONFERENCE ON BIOENCAPSULATION
 Lisbon, Portugal - September 21-23, 2016**

The 24th International Conference on Bioencapsulation was organized in Lisbon Portugal in collaboration with Professor Catarina Reis from Universidade Lusófona de Humanidades e Tecnologias and Prof Luis Fonseca from Instituto Superior Técnico.



The conference took place in the nice auditorium of Lufosona University. The conference dinner took place at the Aura restaurant at the center of Lisbon and was the opportunity for a lot of informal exchanges. The Carpedemicos, a 'musical' group of students, offered a musical and humoristic interlude.



The conference ended by a Fado concert with the singer Beatriz Felizardo, followed by - a wine-cheese tasting. The attendance counted hundred forty participants (24 industrials, 56 researchers and 60 students) coming from



twenty seven different countries. The high industrial attendance demonstrates the attractiveness of the conference, thanks to the high quality of the presented contributions.

Forty oral talks and fifty three posters were presented during the conference. The scientific committee selected ten best oral or poster student presentations (see page 2). Their authors received a diploma and a trophy during the closing ceremony. The abstracts of their contribution are presented in this newsletter issue.



The 2016 Poncelet Innovation Award, supported by Procter and Gamble, was attributed to Doctor Andre Brodkorb from Teagasc Food Research Center, Ireland, both for his contribution to the innovation in the microencapsulation field, and his involvement in the BRG network and activities (see page 2).



During the conference, the General Assembly of the BRG association was held and the minutes are included page 2-3.

Prof. Denis Poncelet
 BRG President

BRG PRIZES AND INNOVATION AWARD

The bioencapsulation research group attributes every years prizes to the 10 best student contributions. The scientific committee, composed of 15 scientific and industrial members, rates all student contributions both orals and posters. The final selection is based on the mean of the 15 scores provided by the scientific committee members.



Luis Fonseca and Catarina Reis, coorganizers of the 2016 BRG conference, Luis Roque, winner of one Best student contribution prize, and Denis Poncelet, BRG president

With the kind sponsorship from Procter & Gamble, since 2011, an award is attributed to a person having contributed strongly to the development of the microencapsulation. The selection is based on open nomination from all BRG members. A selection committee composed of 4 industrials and 4 scientific researchers analyzed the proposal and make the final selection.



Andre Brodkorb, from Teagasc Food Research Center, Ireland, winner of the 2016 Poncelet Innovation Award

BRG GENERAL ASSEMBLY

INTRODUCTION

Each participant was invited to attend the 2016 BRG General Assembly, held at the Annual Conference in Lisbon, Portugal on September 21st, 2016.

2015 ACTIVITY REPORT

Three events were organized by BRG in 2015:

- 7th training School held in Strasbourg University February 23-26, co-organized by Thierry Vandamme from Strasbourg University, France.
- 18th Microencapsulation Industrial Convention, held in Eindhoven, Netherlands April 22-23, co-organized by Nicole Papen Botterhuis from TNO, Netherlands.
- 23th International Conference on Bioencapsulation, held in Delft, Netherlands September 2-4, co-organized by Gabrie Meesters from DSM and Ruud van Ommen from TU Delft, Netherlands.

Table 1 reports the participant and contribution numbers for each event.

Four issues of the BRG newsletter were published in 2015 under the supervision of Paul de Vos from Groningen University (Netherlands) and edited by Brigitte Poncelet from Impascience (France). The newsletter is sent by email to 5000 persons.

- January issue was dedicated to Drug Targeting and Encapsulation and was managed by Thierry Vandamme from Strasbourg University, France.
- May issue presented some of the projects realized over the course of the European Training Network POWTECH, and was supervised by Lilia Ahrne, from SP Food & Bioscience, Sweden.
- Rodrigo Gomez from P&G, Belgium helped to publish the July issue on Industrial applications of microcapsules.

- Best student contributions from 23th International Conference on Bioencapsulation were presented in the November issue.

2015 FINANCIAL REPORT

The 2015 accounting was externally audited by HPL audit, Nantes, France.

A summary of the incomes and expenses is presented in table 2 for each event together with the BRG operating budget. Table 3 presents the cash flow over 2015 it-self. This brings a few remarks

- As expected, the balance for the Strasbourg training school is negative due to the low registration fees and the high number of grants. However, the high level of registration from industry (30%) compensates a large part of from BRG to support the event.
- The Eindhoven convention had a great success with mainly 25 % more participants compared to Brussels 2014, leading to a profit of 28 442 € which largely contributes to the positive balance in 2015.
- The attendance in Delft conference was 10% larger than in Bratislava. Moreover, the industrial attendance was increased by a factor 2.5, again leading to a positive balance.
- In conclusion, 2015 has been a very successful year with regard to the attendances, especially from the industry. All together the cash flow has been increased in 2015 by 22 565 €.

The General Assembly received a report of the annual financial report for 2015 as prepared by HLP auditors. The acceptance of the report was moved by Ron Neufeld (Treasurer) seconded by Paul de Vos. A vote was called and the association was unanimous in accepting the auditor's report.

Table 1 : participation and contributions to the BRG events

	Participants					Contributions		Grants
	Industrials	Reseach.	Students	Exhibitors	Total	Orals	Posters	
Strasbourg	19	17	27	0	63	11	15	27
Eindhoven	70	13	-	16	99	12	-	11
Delft	26	44	52	7	129	40	43	48

BRG EVOLUTION

Following subjects were raised about the strategy of the BRG:

- Registration fees for both training schools and conferences must be kept as low as possible, allowing high participation from students.
- Conference scholarships are attributed by the scientific committee on merit, and based on the quality of the submitted contribution (oral or poster), taking into account the financial and geographical situation of the participant. Question remains how to attribute grants for the training schools.
- One of the objectives of BRG is to promote participation of teams (professor + several students) by offering reduced registration fees to groups.
- Submission of abstracts for the conference needs to be improved to reduce editing manpower. Two options will be evaluated : more advanced word template, and web base submission form.
- The actual BRG newsletter may be replaced by a shorter one based on the "push" approach. This would allow more interactions with the members and diffuse faster information.

STEERING COMMITTEE

The General Assembly elected the following Steering Committee, valid until the next General Assembly to be held in September 2016:

- The only nominee for president was Denis Poncelet from Oniris Nantes France, and the vote was carried unanimously by the members
- The only nominee for treasurer was Ron Neufeld from Queen's University Kingston Canada, and the vote was carried unanimously by the members
- A request for nominations for secretary was presented, and two persons volunteered, Stephane Drusch from TU Berlin Germany and Corinne Hoesli from McGill University Montreal Canada. A vote was called, and both persons were jointly voted
- Paul De Vos was re-elected as co-president and newsletter chief-editor, with support from Brigitte Poncelet

The Steering Committee will be com-

Table 2 : Events and BRG operating budget 2015

	2014 Joao-Pessoa	2015 Strasbourg	2015 Eindhoven	2015 Delft	BRG	Total
registration	2 545 €	20 600 €	106 029 €	49 900 €	950 €	180 024 €
Interests	-	-	-	161 €	354 €	515 €
Receptions	-1 680 €	-12 952 €	-37 502 €	-22 708 €	-	-74 842 €
Printing/mailling	-	-1 963 €	-20 927 €	-2 734 €	-	-25 624 €
Management	-	-6 300 €	-14 190 €	-10 920 €	-2 033 €	-33 443 €
Grants-Missions	-	-5 700 €	-3 443 €	-11 150 €	-	-20 293 €
Bank costs	-	-197 €	-1 525 €	-712 €	-78 €	-2 512 €
Divers	-	-783 €	-	-166 €	-311 €	-1 260 €
Balance	865 €	-7 295 €	28 442 €	1 671 €	-1 118 €	22 565 €
Free registration	-	10 800 €	24 000 €	22 750 €	-	57 550 €

« Grants » corresponds to support offer participants for their travel and accommodation, « Missions » corresponds to the reimbursement of the speakers or chairperson, external financing is funding that has been spend for offering additional grants, all grants and missions get free registration which has to be compensate by BRG.

pleted with the local organizers for the 2017 events.

2016-2017 ACTIVITIES

Three events have been organized in 2016 :

- 19th Microencapsulation Industrial Symposium, Frankfurt, Germany, April 4-6, 2016, co-organized by Thorsten Brandau from Bracke Germany.
- 8th Training School on Bioencapsulation, Cork, Ireland, May 30 - June 2, 2016, co-organized by André Brodkorb from Teagasc Fermoy Ireland and Joanne Fearon from University College Cork Ireland.
- XXIV International Conference on Bioencapsulation, Lisbon, Portugal, September 21-23, 2016, co-organized by Catarina Pinto Reis from University Lusofona and Luis Fonseca from Instituto Superior Tecnico Lisbon, Portugal.
- BRG also helped in organizing a special session at 30th EFFoST International Conference, November 28-30, 2016.

Table 3 : Cash flow over 2015	
End of 2014 balance	56203 €
2014_Joao_Pessoa	865 €
2015_Strasbourg	-7295 €
2015_Eindhoven	28441 €
2015_Delft	1672 €
BRG	-1118 €
Balance	22565 €
End of 2015 balance	78 770 €

Four newsletter issues have been or will be published in 2016 :

- February issue presented some of the oral presentations at the Eindhoven 2015 Industrial Convention
- The May issue was dedicated to Agriculture and Aquaculture, and organized by Amos Nussinovitch from The Hebrew University of Jerusalem Israel.
- The present issue presents the best student contributions at the Lisbon XXIV International Conference on Bioencapsulation.

For 2017, four events are planned:

- 20th Microencapsulation Industrial Convention, Nantes, France, April 10-13, 2017
- 25th International Conference On Bioencapsulation, Nantes, France, June 26-29, 2017
- 9th Training School On Microencapsulation, Berlin, Germany, September 11-14, 2017
- 3rd Latin-America Symposium On Microencapsulation, Pucon, Chile, November 26-29, 2017

CLOSING

As no question were asked by the participants, the General Assembly was closed by the President.

STABILITY AND GASTRO-INTESTINAL DELIVERY OF FOOD BIOACTIVES

Brodkorb, A., Teagasc Food Research Centre Moorepark Fermoy, P61 C996, Co. Cork, Ireland

INTRODUCTION & OBJECTIVES

The concept of “functional food” was developed in Japan over 30 years ago. At the time it was expected that consuming certain types of food may help controlling some disease risk factors especially for the ageing population. Functional foods are not specifically defined or categorised by law and they are regulated through existing food legislation. However, the term functional food is widely used in the market place. It is generally regarded as food that may provide additional functions such as added health benefits beyond its basic, existing nutrition. This further functionalisation of food is commonly achieved by addition of bioactive compounds or organisms. However, health claims are mostly weak and seldom approved by regulatory bodies such as FDA or EFSA. Hence, claims on food packaging are mostly limited to: “lowers your ...”, “improves your ...”, “helps to maintain your ...”, “reduces risk of ...” etc.



A distinctive feature of many bioactive components in food, added or already existing in its natural form, is their vulnerability to harsh environments during food production, storage or gastro-intestinal (GI) digestion. The detrimental consequences of this inherent instability are their degradation and inactivation prior to reaching their target site. For this reason, development of food or food ingredients with bioactive functionalities is an on-going challenge within food research and development. Encapsulation is one method to improve the stability and GI delivery of bioactives in food.

This paper describes approaches used in our group to overcome the limited stability and poor delivery of bioactives such as fatty acids, peptides or bacteria in food.

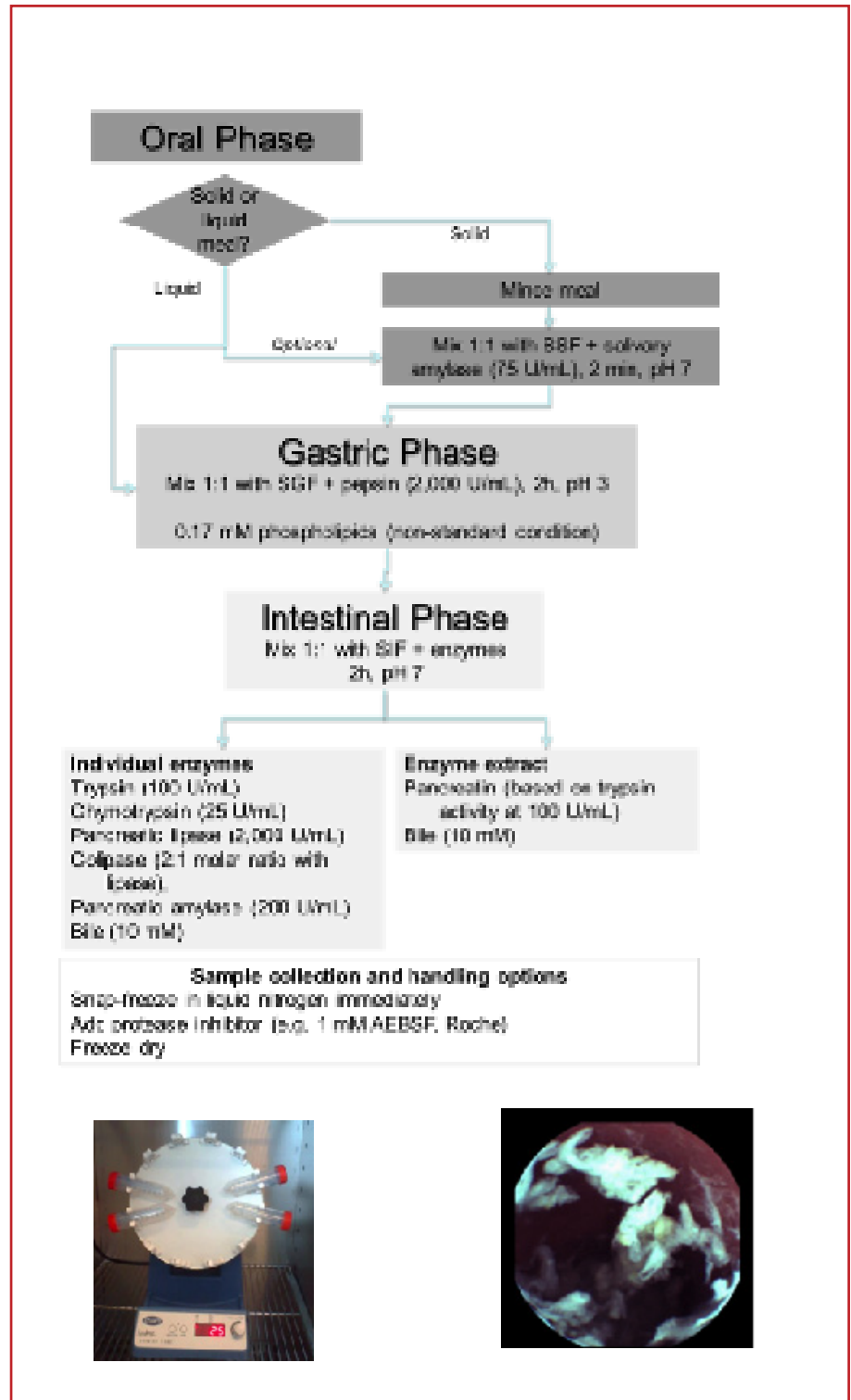


Figure 1. Flow diagram of an international consensus method (INFOGEST method) for standardised in vitro digestion of food². This method differs from comparable pharmaceutical digestion methods e.g. US Pharmacopeia, which are generally unsuitable for monitoring food digestion. Below: Image of the recommended experimental setup for the static INFOGEST digestion methods (left) versus in vivo images of α -lactalbumin digestion in the gastric compartment using wireless capsule endoscopy³.

MATERIALS AND METHODS

Three encapsulation approaches are presented in this paper:

1. Probiotic entrapment in milk protein gels

Probiotic bacteria LGG® (*Lactobacillus rhamnosus* GG ATCC 53103, Valio Ltd., Helsinki, Finland) was encapsulated by entrapment in acid-induced gel beads of heat-denatured whey protein according to Doherty et al.^{1,5}. Beads were formed using a vibrating nozzle droplet encapsulator (Inotech IE-50R Encapsulator®, Inotech AG, Dottikon, Switzerland, now BÜCHI Switzerland). Probiotic release and survival under gastro-intestinal conditions was monitored *in vitro* (static GI digestion method), *ex vivo* (static GI digestion using porcine gastric and intestinal juice) and *in vivo* (porcine model; enumeration in gastric, duodenal, jejunal and ileal content after the sacrificing).

2. Peptide entrapment in starch

Bacteriocines, proteins or peptides produced by bacteria, which can inhibit the growth of similar or closely related bacterial strains, were incorpo-

rated into starch granules after partial heat-induced gelatinisation. Physico-chemical stability of both matrix and the model peptide nisin were evaluated during GI transit. A recently standardised static *in vitro* digestion INFOGEST method for food², described in greater detail below, was used for simulating GI transit. An *in vivo* mouse model was used for assessment of changes in the gut microbiota induced by successful delivery of the bacteriocins. Results are currently compiled and will be published in 2016/2017.

3. Binding fatty acid to native and aggregates of whey proteins:

Oleic (C18:1) and linoleic acid (C18:2) were associated with native α -lactalbumin and β -lactoglobulin and heat-induced aggregates thereof. Non-covalent binding was achieved by slow titration of the more soluble salt of the fatty acids i.e. sodium oleate and linoleate to the protein solution at pH 7. Formation of nano-sized protein particles was achieved by heating the pure whey proteins at defined pH ranges, times and temperature e.g. 80°C for 15 min at pH 5.9, to form highly mono-disperse particles.

A full range of physico-chemical methods was used for characterisation

of the of the encapsulation vehicles, such as static and dynamic light scattering, zeta-potential measurements, SDS-PAGE, HPLC, Nuclear Magnetic Resonance (NMR), confocal laser light microscopy, Scanning and Transmission Electron Microscopy (SEM, TEM), Atomic Force Microscopy (AFM). Bio-accessibility and bio-availability were assessed using the afore mentioned INFOGEST *in vitro* digestion method coupled with assays simulating the intracellular transport of fatty acids into enterocyte-like monolayers (Caco-2)⁴. *In vivo* digestion models included mouse (microbiota), pigs (probiotic release) and adult humans subjects (wireless capsule endoscopy and nasogastric tube sampling)³.



RESULTS AND DISCUSSION

In order to estimate the stability of bioactives during processing, storage and GI transit, standardised methods are required to test their intact nature from both chemical or biological functionality. Simulated gastro-intestinal digestion is widely employed in many fields of food and nutritional sciences, as conducting human trials are often costly, resource intensive, and ethically disputable. As a consequence, *in vitro* alternatives that determine endpoints such as the bioaccessibility and bioavailability of nutrients and non-nutrients, the digestibility of macronutrients (e.g. lipids, proteins and carbohydrates) or release of bioactives from food are used for screening and building new hypotheses. However, various digestion models with vastly different conditions (enzyme assays, kinetics, concentration, dynamic behavior etc.) have been used, often impeding the possibility to compare results across research teams. A recent international consensus was reached within the COST network INFOGEST and resulted in a general standardised and practical static digestion method based on physiologically relevant and available data. For these reason the author highly recommends using the INFOGEST method in order to properly compare and bench-mark results across fields.

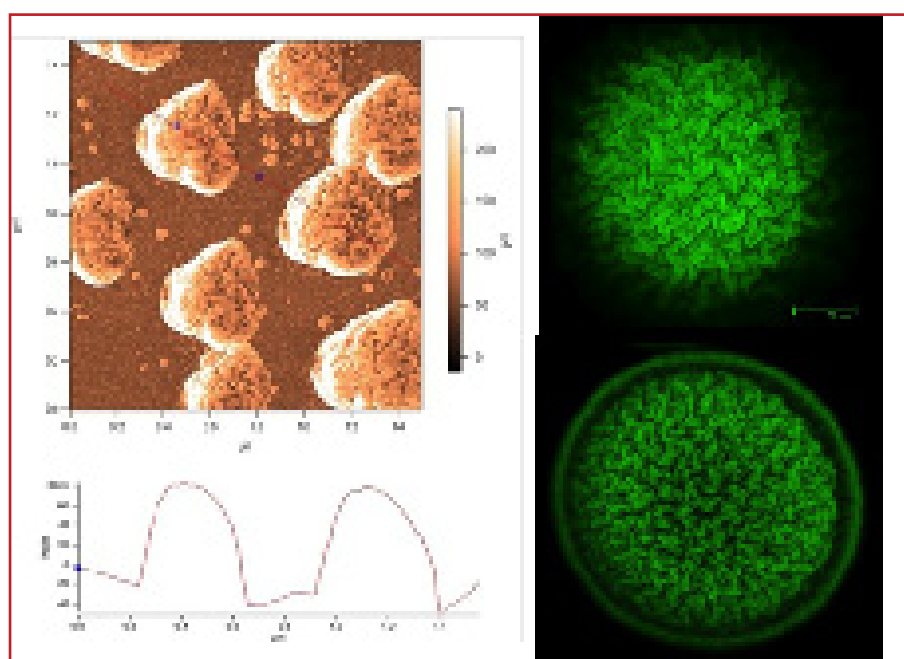


Figure 2. Left: Atomic Force Microscopy (AFM) images ($1.5 \times 1.5 \mu\text{m}$) of whey protein nanoparticles used for protection and delivery of free fatty acids⁴. Right: Confocal LASER light microscopy of whey protein gel beads containing probiotic bacteria¹; upper image focusses on the porous surface topography of the bead, lower image clearly shows an additional polysaccharide coating layer.

ARTICLE

Probiotic survival of LGG® in gelled whey protein isolate (WPI) micro-beads was assessed during ex vivo porcine gastro-intestinal incubation. Free cells showed no survival after 30 min ex vivo stomach incubation (pH 3.4), whereas entrapped cells showed high resistance ($>8.9 \log \text{ cfu/mL}$). This trend was confirmed in subsequent porcine in vivo trials (n=8) using rifampicin-resistant derivative of LGG® where protection in whey protein microbeads increased probiotic viability in the ileum from $7.2 \pm 0.5 \log_{10} \text{ cfu/mL}$ compared to $2.4 \pm 0.4 \log_{10} \text{ cfu/mL}$ for free cells.

Dairy proteins such as α -lactalbumin and β -lactoglobulin are known to form complexes with fatty acids. Due to industrial processing, whey proteins are often in their non-native form in food products, which can modify the FA/protein complex properties. We investigated the interaction of bovine β -lactoglobulin, in selected structural forms (native blg, covalent dimer and as nanoparticles), with sodium oleate (C18:1) and linoleate (C18:2). In the case of linoleate, the stoichiometry fatty acid: protein increased up to 6-fold for nanoparticles (heat-aggregated proteins), compared to that of native β -lactoglobulin. This affected the delivery and subsequent cytotoxicity in Caco-2 cells in the order: free fatty acid > complexed to small dimers > complexed to nanoparticles > complexed to native β -lactoglobulin.

CONCLUSIONS AND PERSPECTIVES

Incorporating labile bioactive ingredients into food requires careful design and formulation of the food components to ensure stability during food processing, storage and GI delivery to the target site. The main limitation for this remains the choice of low-cost food material and processes, which also require consumer acceptance. Natural food components that are already part of the final food product are generally best suited of this purpose, regardless of the size of the encapsulation vehicle.

REFERENCES

1. Doherty, S. B., Gee, V. L., Ross, R. P. et al. Development and characterisation of whey protein micro-beads as potential matrices for probiotic protection. *Food Hydrocolloids* 25, 1604-1617, (2011).

2. Minekus, M., Alming, M., Alvito, P. et al. A standardised static in vitro digestion method suitable for food - an international consensus. *Food & Function* 5, 1113-1124, (2014).
3. Sullivan, L. M., Kehoe, J. J., Barry, L. et al. Gastric digestion of α -lactalbumin in adult human subjects using capsule endoscopy and nasogastric tube sampling. *Br. J. Nutr.* 112, 638-646, (2014).
4. Le Maux, S., Brodkorb, A., Croguennec, T. et al. β -Lactoglobulin-linoleate complexes: In vitro digestion and the role of protein in fatty acids uptake. *Journal of Dairy Science* 96, 4258-4268, (2013).
5. Doherty, S. B., Auty, M. A., Stanton, C. et al. (2012). Survival of entrapped *Lactobacillus rhamnosus* GG in whey protein micro-beads during simulated ex vivo gastro-intestinal transit. *International Dairy Journal*, 22(1), 31-43.



Dr André Brodkorb

Teagasc Food R. C.
Food Chemistry & Technology Dep.
Fermoy Co. Cork - Ireland
andre.brodkorb@teagasc.ie

Dr André Brodkorb is a graduate of chemistry of the Friedrich Schiller University Jena, Germany with a PhD in bio-physical chemistry from the Université Libre de Bruxelles, Belgium. He is a senior researcher in colloidal and protein chemistry in the Teagasc Food Research Centre in Moorepark, Ireland. His main research interest is in the area of structure, aggregation, gelation and functionalities of food proteins and their application in nutritional product. Some of the more recent work dealt with process-induced changes in food structure and their effect on the fate of food during gastro-intestinal transit in vitro and in vivo. This experience in structuring of food or food components was applied for the development of encapsulation devices for the delivery of small bioactive food components but also larger probiotic bacteria in microgels. Dr Brodkorb is the author of over 50 peer-reviewed papers and two patents.

LOOKING FOR AN INDUSTRIAL POSITION



I am a Master's candidate in Chemical Engineering at McGill University in Canada, and I will be completing my studies in December. My Master's research, supervised by Professor Corinne Hoesli, was focused on developing microchannel emulsification for islet encapsulation for the cell-based treatment of diabetes. This interdisciplinary project required expertise in a variety of fields, including mammalian cell culture, fluid dynamics, and encapsulation technologies.

I have also participated in several BRG events, including the 7th Training School on Microencapsulation (Strasbourg, 2015) and was winner of the best student contribution in 2017 at the 24th International conference on bioencapsulation.

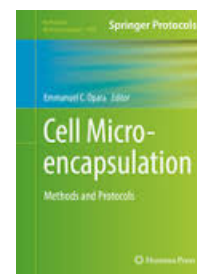
I am currently looking for an industrial position in the pharmaceuticals, food, or cosmetics field for early 2017, and I am open to relocating anywhere for the position.

To contact me

karen.markwick@mail.mcgill.ca

BOOK

Cell Microencapsulation :Methods and Protocols



Editors: Opara, Emmanuel C. (Ed.) Humana Press Inc. (Verlag)
<http://www.springer.com/us/book/9781493963621>

Ebook (\$65.40)
ISBN 978-1-4939-6364-5
Harcover (\$84,40)
ISBN 978-1-4939-6362-1



Special session organized by BRG

<http://www.fffostconference.com/special-sessions.asp>



20th Microencapsulation Industrial Convention



Nantes, France

April 10-13, 2017



http://Bioencapsulation.net/2017_Nantes_i

25th International Conference on Bioencapsulation



Nantes, France
June 26-29, 2017



http://Bioencapsulation.net/2017_Nantes_c



21st International Symposium on Microencapsulation

Faro Algarve, Portugal
September 27-29, 2017

<http://ismicroencapsulation2017.ualg.pt>

IXth Training School on Microencapsulation



Berlin, Germany
September 11-14, 2017



http://Bioencapsulation.net/2017_Berlin

3rd Latino-America Symposium on Microencapsulation



Pucon, Chile
November 27-29, 2017



http://Bioencapsulation.net/2017_Pucon

MAGNETIC LIPOSOMES FOR REMOTE CONTROLLED RELEASE OF ANTICANCER DRUG

Petrinin A^{1,2}, Gileva A¹, Vlasova K², Akasov R¹, Golovin Yu^{2,3}, Majouga A^{2,4}, Klyachko N², Markvicheva E¹

INTRODUCTION AND OBJECTIVES

Magneto-mechanical approach to remote controlled drug release is promising due to its high specificity, versatility and locality [1]. Recently, theoretical and experimental assays showed that non-heating low-frequency (LF) magnetic field (MF) can be used in various biomedical applications. Thus, controlled drug release from nanocarriers or polymeric shell of the functionalized magnetic nanoparticles (MNPs), the control of enzymatic reaction kinetics as well as possibility to affect functions of alive cells by stimulating cell membrane structures (ionic channels) or receptors could be mentioned. Theoretical models and calculations demonstrated that MNPs exposed to easily generated in laboratories magnetic fields ($B < 1T$) can induce force values up to several hundred piconewtons. According to the results of single-molecule force spectroscopy, these forces can induce significant deformations in macromolecules, and, as a result, to change their properties. Therefore, functions of bioactive molecules can be manipulated. Moreover, MNPs attached to these macromolecules or drug loaded nanocontainers can promote disordering the nanocontainer shell, and thereby to provide controlled drug release under LF MF exposure (Fig. 1).

In recent years, progress in MNPs technologies led to development of magnetic nanoformulations, including

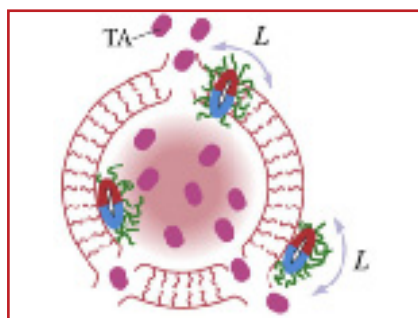


Figure 1. Scheme of MNPs possible localisations in/on a nanocarrier. TA is a therapeutic agent and L is the torque applied to the MNP.

liposomes. These magnetic liposomes (MLs) fabricated from thermosensitive polymers could be activated by high frequency MF, i.e. using the effect of hyperthermia caused through magnetic particles. In this case, high-frequency (high intensity) magnetic field is used during a long time which makes the method inconvenient. Our research deals with calculations of optimal parameters of the non-heating MF in order to provide remote controlled drug release from nanocontainers loaded with magnetic nanoparticles.



Thymoquinone (TQ), which was selected here as a model lipophilic drug, is the main active component of black seed essential oil. It was found to possess both anti-inflammatory and anti-cancer effects due to inhibiting both tumor metastasis and angiogenesis [2].

The aim of the study was to fabricate magnetic liposomes loaded with thymoquinone and/or Nile Red, to study their accumulation in tumor cells and to evaluate the effect of low-frequency magnetic field on model drug release.

MATERIALS & METHODS

Nile Red (NR) dye, Hoechst 33258, TQ, egg lecithin, fluorescein and cholesterol were from Sigma-Aldrich. Ammonium salt of 1,2-distearoyl-sn-glycero-3-phosphoethanolamine-N-[amino(polyethylene glycol)-2000 (DSPE-PEG) was from Avanti Polar Lipids (USA). DMSO (99.5%), PBS (pH 7.4), 0.25% (v/v) trypsin-EDTA solution, Dulbecco's modified Eagle's medium (DMEM) and fetal bovine serum (FBS) were from PAN-Biotech (Germany), magnetite particles (Fe₃O₄) were kindly provided by Dr. M. Abakumov (MSU, Moscow).

Magnetic liposomes preparation & characterization

Liposomes were prepared as follows: MNPs, TQ (or NR), egg lecithin and

phosphatidylcholine were dispersed in chloroform, dried to get a thin film and then dispersed in PBS (pH 7.4). Finally, sonicated and free MNPs were separated by passing the emulsion through an extruder with pore size filter of 400 nm. Some samples contained also other components, namely DSPE-PEG or cholesterol, which were added to the mixture before dissolving in chloroform. A drug excess was removed using NAP-25 desalting column. TQ loading (2 wt %) was determined by HPLC. MNPs concentration (4 wt %) was calculated from iron content (FerroZine assay kit). The size of MLs was measured by Zetasizer Nano ZS, Malvern (UK) and using TEM (LEO 912 ABOMEGA Carl Zeiss, Germany).



Cell culture

Human breast adenocarcinoma MCF-7 cells were cultivated in DMEM supplemented with 10% FBS in a 5% CO₂ humidified atmosphere at 37°C. The cells were detached after treatment with a 0.25% (v/v) trypsin-EDTA solution, and the culture medium was replaced every 3-4 days.

Confocal microscopy

The cellular uptake and localization of MLs was observed by confocal laser microscope (Nikon TE-2000, Japan). For this purpose, MLs previously loaded with NR dye, were incubated with MCF-7 cells in DMEM in the CO₂-incubator for 5 min and 1 h. To visualize nuclei, the cells were stained with Hoechst 33258 (50 μM, 10 min). Then the cells were washed three times with PBS (pH 7.4), fixed with a CC/Mount fluorophor protector and observed by confocal microscopy. Excitation wavelength values were 543 nm for NR and 360 nm for Hoechst 33258, while fluorescence signals were collected at 560-650 and 380-460 nm for NR and Hoechst 33258, respectively.

ARTICLE



Figure 2. TEM image of MLs loaded with MNPs. Scale bar is 100 nm.

RESULTS & DISCUSSION

Magnetic liposomes preparation and characterization

Base components of the MLs were egg lecithin, cholesterol and MNPs. To study accumulation of MLs in tumor cells, TQ and/or NR were added. The effect of liposome PEGylating was explored by adding DSPE-PEG. Fluorescein was entrapped in the MLs to study the effect of LF MF on model drug release.

Physico-chemical properties of magnetic liposomes

A mean diameter of magnetic liposomes loaded with TQ and/or NR was 160 ± 14 nm, while polydispersity index (PDI) was 0.25 ± 0.10 . The liposomes were stable in Milli Q and PBS (pH 7.4) at least for one month at 40 °C and for 1 week at 37 °C. According to TEM images, MNPs were located in the inner part (a core) of the MLs (Fig. 2). After exposure of MLs samples for 3 and 25 min to MF, the MNPs aggregated into clusters and then rotation of these clusters has destroyed the liposome membrane. As was shown by IR-spectroscopy, the MF application caused "melting" the MLs membrane, while the "melting" range depended on MF exposure time and MF intensity. For example, in case of MF intensity of 50 Hz, the membrane "melting" started in 5 min of the exposure, while the maximum peak shifting was found after 15 min. Then the effect decreased, which could be explained by MLs damage. These results are in a good agreement with those obtained from release experiments.

Fluorescein release from magnetic liposomes

MLs obtained from lecithin, MNPs and cholesterol (4 wt %), were loaded with

hydrophilic fluorescein. The release experiments were carried out using dialysis system. Under external MF conditions, the release was found approx 80% for 40 min compared to 45% in a control sample (without MF). Moreover, in the case of MF exposures, fluorescein was mostly released for the first 10 min. It could be explained by rather fast destruction and/or reorganization of the lipid bilayer.

Accumulation of liposomes in tumor cells

Accumulation and distribution of liposomes loaded with NR in MCF-7 cells are shown in Fig. 3. After 5 min incubation, the MLs were found to occur on the cell membrane and in the cytoplasm. After the incubation for 1 h, the MLs distribution in the cells was more heterogeneous: MLs were mostly located in the cell organelles around the cell nucleus, most probably in the endoplasmic reticulum. However, additional experiments are needed to confirm this hypothesis.

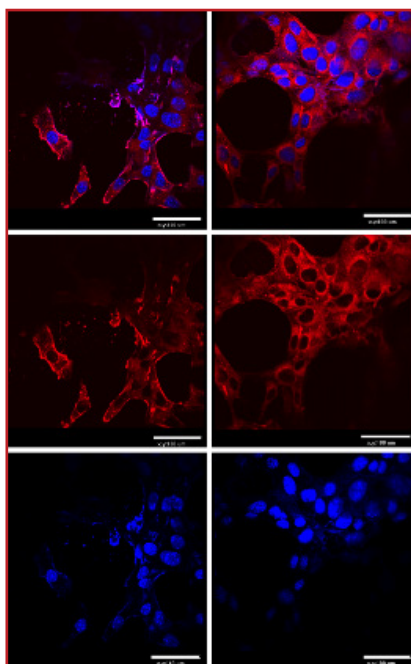


Figure 3. Accumulation of MLs in MCF-7 cells in 5 min (the left panel) and 1 h (the right panel). Cell nuclei (in blue) were stained with Hoechst 33258, MLs (in red) were loaded with Nile Red dye. Scale bar is 50 μ m.

CONCLUSIONS AND PERSPECTIVES

MLs were obtained and characterized. Evaluation of release kinetics of fluo-

rescein from MLs showed that use of external LF MF could accelerate drug release due to destruction and/or reorganization of the liposome lipid bilayer. Cell uptake of MLs loaded with NR was studied using human breast adenocarcinoma MCF-7 cells. The *in vitro* cytotoxicity studies of MLs loaded with TQ under LF MF are in progress.

REFERENCES

1. Golovin Y., Gribovsky S., Golovin D., Klyachko N., Majouga A., Master A., Sokolsky M., Kabanov A., Towards nanomedicines of the future: Remote magneto-mechanical actuation of nanomedicines by alternating magnetic fields // *J. Contr. Release*, 2015, 219: 43-60.
2. Racoma I., Meisen W., Wang Q., Kaur B., Wani A., Thymoquinone Inhibits Autophagy and Induces Cathepsin-Mediated Caspase-Independent Cell Death in Glioblastoma Cells // *PLoS One*, 2013, 8, e72882.



Alexander Petrunin

Shemyakin-Ovchinnikov Institute of Bioorganic Chemistry
Russian Academy of Science
Moscow, Russia
buttonightwedance45@gmail.com

Acknowledgements

Grant support: RSF 14-13-00731 (MF experiments)

¹ Shemyakin-Ovchinnikov Inst. Bioorg. Chem., Rus. Acad. Sci., Moscow, Russia

² Lomonosov Moscow State University, Moscow, Russia

³ Derzhavin Tambov State University, Tambov, Russia

⁴ National University of Science and Technology "MISIS", Moscow, Russia

ENCAPSULATION OF ENDOPHYTIC *M. BRUNNEUM* FOR BIOLOGICAL CROP PROTECTION

Krell, V.¹, Jakobs-Schoenwandt, D.¹, Vidal, S.², Patel, A. V.¹ - Bielefeld University of Applied Sciences, Germany

INTRODUCTION AND OBJECTIVES

Fungi like *M. brunneum* spp. are promising biocontrol agents that are pathogenic to many different insect orders and are able to endophytically colonize different plant species and plant parts paving the way for novel plant protection measures (Vidal and Jaber, 2015). However, biocontrol of insect pests with these fungi is challenging because of the low efficacy, difficult application, limited survival after drying and shelf life of the usually insufficiently formulated "active ingredient".

Therefore, the objective of the current investigation was to encapsulate *M. brunneum* BIPESCO 5 hyphal bodies in an optimized bead formulation and to deliver the fungus to tomato plants to support plant colonization via the roots for a systemic protection from herbivorous insects, such as whiteflies. Moreover, the formulation should be stable during drying and storage for a period of six months.



MATERIALS & METHODS

To investigate the impact of formulation on *M. brunneum* BIPESCO 5 hyphal bodies, fungal biomass was selectively produced in shake flasks in a medium based on agricultural residues and osmotic stress inducers. For bead production, 2 % sodium alginate (w/w), 20 % corn starch (w/w) and 1.5% biomass (w/w) were dripped into 2 % calcium chloride solution (w/v) and cross-linked for 20 min. Drying of beads was accomplished in a self-constructed vacuum drying apparatus at 30 °C for 3 d to an $a_w \leq 0.1$.

Prior to the plant colonization assay, mycelial growth from beads was ana-

lyzed. Therefore, moist and dry beads were incubated on sterile and non-sterile soil for 14d at room temperature and the radial mycelial length was measured. To investigate plant colonization, beads were applied to tomato plant roots (BBCH 14) and colonization was analyzed in the stem with a duophasic approach using light microscopy and qPCR after three weeks.

For real time storage tests over a period of six months, three different temperatures were chosen, namely 25 °C, 18 °C and 5 °C to simulate different storage conditions. Dry beads were wrapped in oxygen and -moisture impermeable aluminium/polyethylene bags (5x5cm). Viability of hyphal bodies was determined by counting the colony forming units after dissolving of beads in a buffered citric acid solution and spreading diluted samples on SDA plates followed by an incubation at 25 °C for 4 d.

Statistical analyses were carried out with the software SPSS version 22. For percentage values, data was arcsine-square-root transformed prior to analysis. All values are given as means \pm standard deviation.

RESULTS & DISCUSSION

Drying

Viability of encapsulated hyphal bodies after drying was significantly increased from 0.7 ± 0.5 % for unformulated hyphal bodies to 51.9 ± 3.5 % for encapsulated fragments ($t_6=31.2$; $P<0.001$).

Mycelial growth

As a prerequisite for the plant colonization assay, we assessed whether

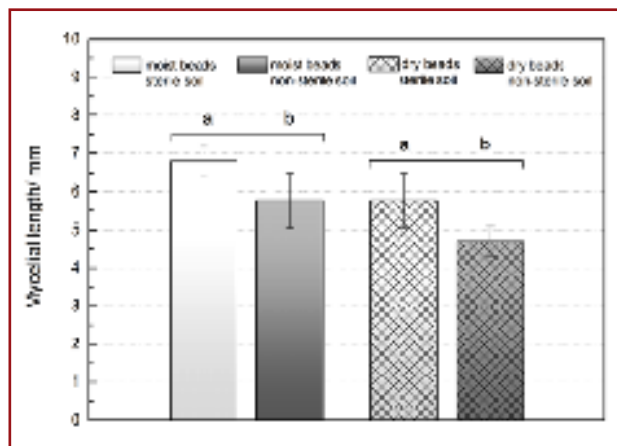


Figure 1. Growth of mycelia from Ca-alginate starch beads (moist: $a_w=0.967 \pm 0.018$, dry: $a_w=0.105 \pm 0.011$) with encapsulated hyphal bodies after 14 days (n=5). Different letters above bars show significant differences according to two-sample t-test at $P<0.05$.

encapsulated hyphal bodies were able to grow out of beads on non-sterile soil in competition with other microorganisms and their metabolites (Figure 1).

As expected, mycelial growth from moist beads was increased compared to dry beads. Furthermore, for both dry and moist beads, there was an inhibition of mycelial growth on non-sterile compared to sterile soil. Although this difference was significant, results were still satisfying since a strong inhibition by the soil-borne microbial community has been shown for other entomopathogenic fungi, such as *B. bassiana* (Lohse et al., 2015).



Plant colonization

Tomato plant roots were treated with beads to investigate whether plant colonization via the root system with encapsulated hyphal bodies could be accomplished. In addition, unformulated hyphal bodies with the same dosis of active biomass as in moist beads were applied to look into the benefit of encapsulation for colonization.

ARTICLE

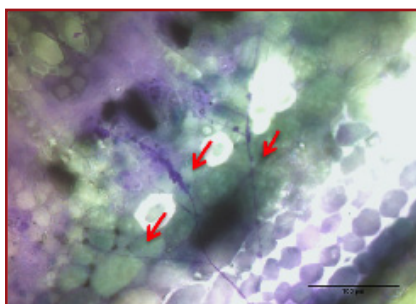


Figure 2. Cross section of a tomato stem for microscopic analysis of endophytic hyphae quantity stained with Rose-Bengal (x200)

When plant roots were treated with beads, significantly more hyphae were quantified compared to control plants (Figure 2, Figure 3; $F_{3,99}=133.1$; $P<0.001$). After application of dry beads, the number of endophytic hyphae was increased 7.6 fold. With moist beads, colonization was enhanced 23.4 fold compared to control plants. Application of unformulated moist hyphal bodies resulted in a similar colonization as with dry beads. Because of the protective effect of the bead, better colonization was hypothesized with dry beads compared to unformulated hyphal bodies. However, after drying, viability of hyphal bodies decreased by almost 50 % thus probably being responsible for less successful colonization. Furthermore, dried encapsulated hyphal bodies have a growth disadvantage since beads and cells have to rehydrate. In addition to microscopic analyses, colonization for all treatments was confirmed by qPCR.

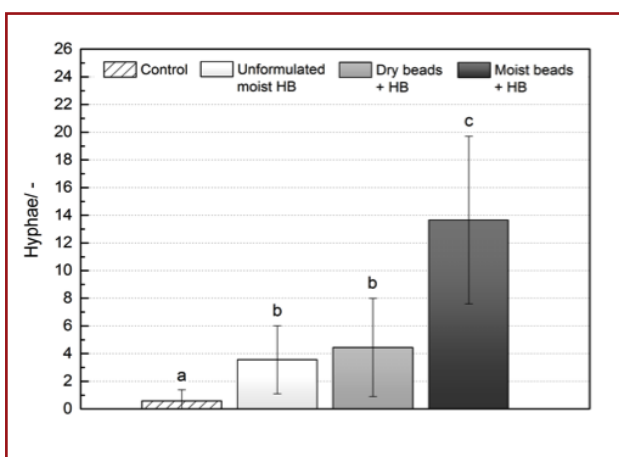


Figure 3. Tomato plant colonization after application of formulated and unformulated *M. brunneum* BIPESCO 5 hyphal bodies (n=25). Different letters above bars show significant differences according to ANOVA and Bonferroni post hoc test at $P<0.05$. HB: hyphal bodies

Shelf life

To investigate whether beads with encapsulated hyphal bodies could be stored for a period of six months, real-time storage tests were conducted. Since cold storage is costly and not always available, higher storage temperatures (18°C, 25°C) were tested as well (Figure 4).

After six months, dry encapsulated hyphal bodies maintained viability with 64.4 ± 14.5 % at 5°C, 44.8 ± 10.8 % at 18 °C and 32.5 ± 2.1 % at 25 °C. Interestingly, there was no significant difference between shelf life at 5 and 18 °C. However, shelf life was significantly reduced when hyphal bodies were stored at 25 °C compared to 5 °C but not compared to 18 °C ($F_{2,8}=7.6$; $P<0.05$).

CONCLUSIONS

Survival after drying of *M. brunneum* BIPESCO 5 hyphal bodies was substantially improved by encapsulation in Ca-alginate starch beads. Furthermore, the formulation enabled fungal growth out of beads and colonization of plant tissue after application of beads on tomato plant roots was found to be highly efficient. In addition, encapsulated *M. brunneum* BIPESCO5 hyphal bodies exhibited good shelf life at 5 and 18 °C after six months.

On-going experiments are looking into endophytic insect virulence against herbivorous insects on tomato and potato plants. In addition, further beneficial effects of the formulation, such as plant growth promotion, will be evaluated.

REFERENCES

- Vidal, S., & Jaber, L. R. Entomopathogenic fungi as endophytes: plant-endophyte-herbivore interactions and prospects for use in biological control. *CURRENT SCIENCE* 108, 1 (2015).

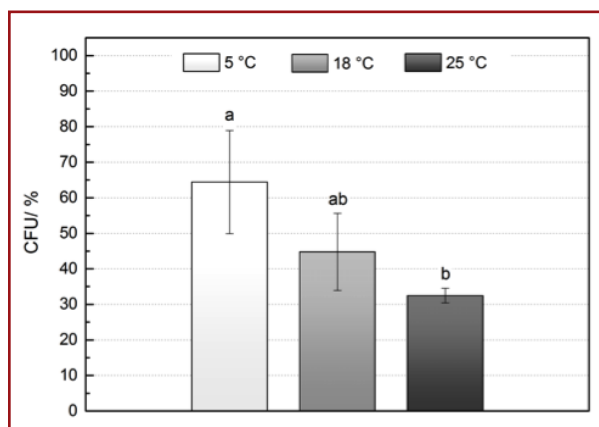


Figure 4. Shelf life of encapsulated hyphal bodies stored for six months at 25 °C, 18 °C and 5 °C (n=4). Different letters above bars show significant differences according to ANOVA and Bonferroni post hoc test at $P<0.05$. CFU: colony forming unit

- Lohse, R., Jakobs-Schoenwandt, D., Vidal, S., & Patel, A. V. Evaluation of new fermentation and formulation strategies for a high endophytic establishment of *Beauveria bassiana* in oilseed rape plants. *Biological Control* 88, 26-36 (2015).



Vivien Krell

Bielefeld University of Applied Sciences
Engineering Sciences and Mathematics
Bielefeld - Germany
vivien.krell@fh-bielefeld.de

Acknowledgements

This research was funded by the German Federal Environmental Foundation (FKZ: 3142/01). We thank Hermann Strasser (University Innsbruck) for providing the isolate *M. brunneum* BIPESCO 5.

¹Bielefeld University of Applied Sciences, Department of Engineering Sciences and Mathematics, Interaktion 1, 33619 Bielefeld, Germany
²Georg-August-University Goettingen, Department of Crop Sciences/Agricultural Entomology, Grisebachstr. 6, D-37077 Goettingen, Germany

MICROCHANNEL EMULSIFICATION: A NOVEL APPROACH TO CELL ENCAPSULATION

Markwick, K.E.¹; Dussault, M.A.²; Bégin-Drolet, A.²; Hoesli, C.A.¹

INTRODUCTION AND OBJECTIVES

Transplantation of encapsulated pancreatic islet cells is a promising method to treat type 1 diabetes without the need for chronic immune suppression post-transplantation. The most common material used for islet cell encapsulation is alginate, a biocompatible, anionic hydrogel. Hoesli et al.¹ adapted an emulsification and internal gelation method originally described by Poncelet et al.² for beta cell encapsulation. The modified stirred emulsification process can be used to generate beads from very concentrated, viscous alginate solutions, leading to beads with reduced antibody permeability. However, the alginate beads are polydisperse in size, which may lead to diffusion limitations in larger beads and improper cell encapsulation in smaller beads³.



Microchannel emulsification (MCE) was first proposed by Kawakatsu et al.⁴ as a novel method to produce regular-sized droplets of both oil-in-water and water-in-oil emulsions. The droplet generation in MCE is driven by interfacial tension forces, hence requires no shear stress as well as little energy input. The to-be-dispersed phase flows through microchannels in a thin plate, forming droplets into the continuous phase at the exit of the channels (Figure 1). Microchannels (MCs) can be fabricated as either grooved MCs with a terrace or straight-through micro-

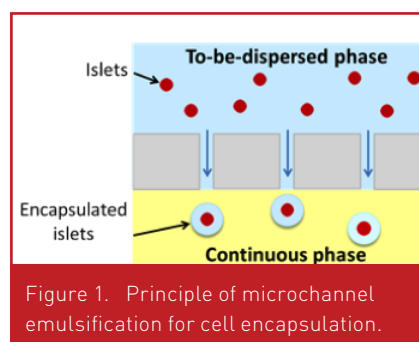


Figure 1. Principle of microchannel emulsification for cell encapsulation.

channels. Straight-through microchannels have the advantage of significantly higher droplet formation rates compared to grooved microchannels. To produce monodisperse droplets, the continuous phase must preferentially wet the surface of the microchannel plate. When using alginate as the dispersed phase, a hydrophobic plate with a water contact angle $> 90^\circ$ should be used. MCE has now been used to produce uniform emulsions with dispersed phase droplets ranging from microns to millimetres in diameter with coefficients of variation (C.V.) of $< 5\%$, at production rates up to 1.4 L/h^5 .

The objective of this work was to develop microchannel emulsification as a means to produce uniformly sized alginate beads for encapsulated islet transplantation applications. The microchannel emulsification equipment was developed and the operating procedure was designed. Preliminary studies of the effects of operating parameters on alginate bead production were conducted. Microchannel emulsification was chosen as an encapsulation method so as to produce highly concentrated, uniform alginate beads at clinically relevant production rates.

MATERIALS & METHODS

Autodesk AutoCAD and SketchUP software were used to design the microchannel plates. Microchannel plates with oblong channels were then 3D printed by Shapeways 3D Printing service using an acrylic polymer. Microchannel plates with circular channels were produced by 3D printing a mold of the desired channels from sugar, and then pouring silicon in the mold. Once set, the sugar was dissolved, leaving the desired channels.

Alginate beads were produced using a preliminary microchannel emulsification set up. Two flow chambers, for the alginate and oil, were made from polycarbonate, with inlet and outlet tubing on either side. The microchannel plate was placed between the



two chambers. A 1.5% alginate solution was prepared, as well as mineral oil acidified with acetic acid. A Sage Instruments model 355 syringe pump was used to pump the alginate at flow rates from $2 - 70 \text{ mL/min}$. A Harvard Apparatus PHD 2000 Programmable syringe pump was used to pump mineral oil at flow rates from $0 - 85 \text{ mL/min}$. The bottom oil chamber was filled with oil, and the top alginate chamber then filled with alginate. The alginate outlet tubing was then clamped, and both the alginate and oil flows started. The alginate passed through the microchannels and formed droplets into the flowing oil. The alginate droplets and oil outlet were collected in a beaker.

Collected beads were stained with saturated toluidine blue solution in medium for 60 minutes on a rotary shaker at 40 rpm. The beads were transferred to a Petri dish and an image acquired using a Samsung Galaxy S4 13MP camera. CellProfiler image analysis freeware (www.cellprofiler.org/) was used to determine the bead sizes. .

RESULTS & DISCUSSION

First attempts to produce an emulsion using MCE resulted in jetting visualised as a continuous outflow and expansion of the alginate (Figure 2A). Modification of the process parameters, including alginate and oil flow rates, surfactant type and concentration, and microchannel dimensions resulted in the production of uniform, spherical droplets of alginate beads (Figure 2B), in the range of $3 - 5 \text{ mm}$ in diameter.

Table 1: Microchannel plate properties

	Material	Water contact angle ($^\circ$)	Channel hydraulic diameter (μm)	Channel aspect ratio	Channel length (mm)
MC1	Acrylic polymer	70	311	3.5	1
MC2	Silicon	95	750	1	4

ARTICLE

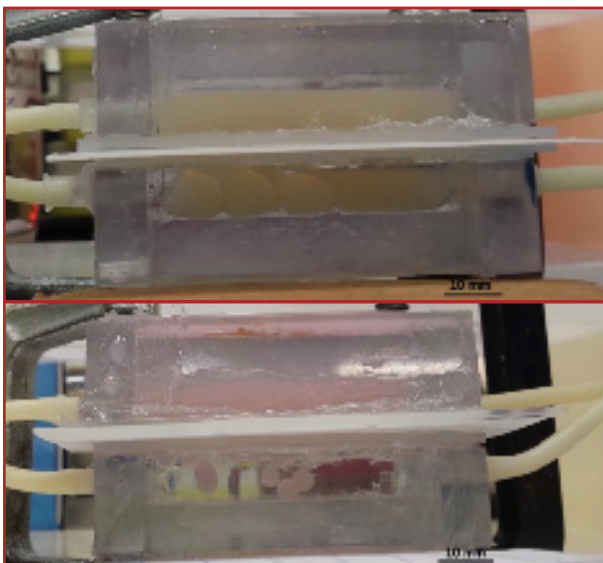


Figure 2. (A) Microchannel emulsification before process modification shows jetting of the alginate. (B) Microchannel emulsification after process parameter shows uniform bead production.

Two different microchannel plates with different properties, MC1 and MC2, were tested with microchannel emulsification (Table 1).

The MC1 plate produced beads that were, on average, ~3 mm in diameter. The MC2 plate produced beads that were 4.9 ± 0.3 mm in diameter, corresponding to a coefficient of variation of 5.4 % (Figure 3). The large diameter alginate beads took approximately 45 minutes to fully gel; as a result, most

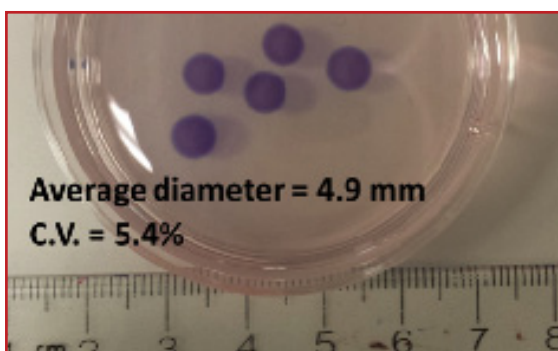


Figure 3. Alginate beads produced by MCE with MC2.

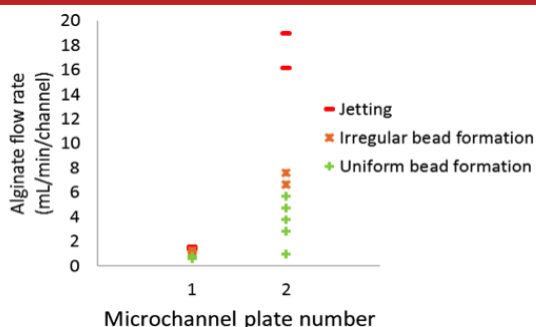


Figure 4. State diagram of bead production by MCE.

of the beads coalesced before complete gelation. Increasing the space between adjacent microchannel reduced coalescence.

Three flow regimes were observed with increasing dispersed phase flow: uniform bead formation, irregular bead formation, and jetting. The uniform bead formation regime exists below a critical capillary number, where interfacial tension is the dominant force driving droplet formation. Above the critical capillary number, viscous force effects become significant. The flow behaviour was tested with varying alginate flow rates using both MC1 and MC2 plates

(Figure 4). Uniform bead formation was observed at higher channel flow rates, hence higher capillary numbers, with MC2 than with MC1.

It was expected that a more robust uniform bead formation operating range could be obtained by increasing the MC material hydrophobicity, the channel aspect ratio, or the channel length. It was observed that MC2, with a higher water contact angle and longer channel length, resulted in a larger uniform bead formation range than MC1, with a higher channel aspect ratio.

CONCLUSIONS

Microchannel emulsification presents a promising technique to encapsulate pancreatic cells in uniform, high-concentration alginate at high production rates. Alginate beads of 3 – 5 mm diameter can be produced with a coefficient of variation of ~5%. Future work will include factorial design to optimize the microchannel plate design and operation parameters to obtain alginate beads of 600 μ m in diameter. It is expected that reducing the bead size will reduce bead coalescence due to the reduced gelation time. The physicochemical properties of the beads will then be characterized, inclu-

ding size, circularity, surface roughness, strength, and stability. Mouse Insulinoma 6 (MIN6) cells will then be encapsulated using the microchannel emulsification process. Cell recovery, cell survival, as well as glucose-responsive insulin secretion will be assessed. This work demonstrates the feasibility of using microchannel emulsification for the production of alginate beads at production rates sufficient for potential clinical islet transplantation applications.

REFERENCES

- Hoesli, C. et al. Pancreatic Cell Immobilization in Alginate Beads Produced by Emulsion and Internal Gelation. *Biotechnology and Bioengineering* 108, 424–434 (2011).
- Poncelet, D., Lencki, R., Beaulie, C. & Neufeld, R. J. Production of alginate beads by emulsification/internal gelation. 1. Methodology. *Appl. Microb. Biotechnol.*, 39–45 (1992).
- De Vos, P., De Haan, B., Pater, J., & Van, S. R. Association between capsule diameter, adequacy of encapsulation, and survival of microencapsulated rat islet allografts. *Transplantation*, 62, 893–9 (1996).
- Kawakatsu, T., Kikuchi, Y., & Nakajima, M. Regular-sized cell creation in microchannel emulsification by visual microprocessing method. *Journal of the American Oil Chemists' Society*, 74, 317–321 (1997).
- Kobayashi, I., Uemura, K., & Nakajima, M. Effect of channel and operation parameters on emulsion production using oblong straight-through microchannel arrays. *Japan J. Food Eng.*, 10, 69–75 (2009).



Karen Markwick
McGill Univ.
Chemical Engineering
Montreal Quebec - Canada
karen.markwick@mail.mcgill.ca

Acknowledgements

NSERC, FRQNT, Diabète Québec, Thé-Cell, CQMF, and the Eugenie Ulmer Lamothe Fund for their financial support.
¹.McGill University, Canada.
².Université Laval, Canada.

CUSTOM-TAILORED SOL-GEL DERIVED MATRICES FOR CHEMICALS' IMMOBILIZATION

Loureiro, M., Lourenço, M.J. – FCUL-UL (CQE) - Marques, A.C., Bordado, J.C., IST-UL (CERENA), Portugal

INTRODUCTION AND OBJECTIVES

Organic compounds have been widely used as an encapsulating material, but polymer-based microspheres (MSs) usually suffer from poor chemical and physical stability [1]. Therefore, a great deal of research has been devoted to inorganic metal oxide microparticles, which provide chemical resistance and thermal and mechanical stability to the MSs.



The increased interest in inorganic microcapsules is also due to their distinct characteristics, such as the non-toxic quality for the environment, biocompatibility and the ability to easily incorporate additional functional groups, which enables the use of these structures in a variety of applications [1-2].

Sol-gel technology combined with the microemulsion method has been shown to be the most effective and economical technique for silica-based microspheres, microcapsules and other matrices' synthesis. This method allows the synthesis of both inorganic and hybrid structures, while still providing the control of the particles' microstructure and the typical low processing temperatures, consisting of a versatile and cost-saving process [2].

In this work, inorganic silica or organic functional silica based MSs have been developed, using sol-gel processing technology in combination with the microemulsion technique. Tetraethyl orthosilicate (TEOS), [3-Glycidyoxypropyl] trimethoxysilane (GPTMS) and methyltriethoxysilane (MTES) were used as biocompatible Si precursors for the MSs' synthesis. Therefore, it is possible to use the obtained MSs as matrices for immobilization or entrapment of some biomolecules or chemicals for bio-applications.

The present work regards the development of MSs, or matrices, with different types of organic functionality, different degrees of porosity, morphology and size, tuned for the encapsulation of different sized molecules and their controlled release. They have been characterized by Scanning Electron Microscopy (SEM) and Fourier Transformed Infrared Spectroscopy (FTIR). These MSs have been developed in the framework of the Microencapsulation Technology Platform at IST and have shown a great potential to encapsulate water, glycerol, amines, etc. We are now open to test them with selected chemicals or biomolecules.

MATERIALS & METHODS

Materials

TEOS (99%), MTES (99.5%) and GPTMS (>98%) were purchased from Dow Corning. The organic solvent and the surfactant, SPAN80 (99%) were purchased from Merck KGaA, and used as received, without further purification.

Synthesis of the microspheres or matrices

Inorganic silica MSs: Water-in-oil (W/O) emulsion solution was obtained through homogenization of the water and oil phases with the use of an Ultra-Turrax (IKA) dispersing device. SPAN80 was used as emulsifier for the emulsion system formation and stability purposes. An aqueous mixture of acidified water and TEOS were stirred at 100 rpm for one hour at room temperature. Both the emulsion and the pre-hydrolyzed silane solution were mixed for one hour at 600 rpm at room temperature, in a reaction balloon. Afterwards, the temperature was increased by steps up to 80°C. The obtained MSs were subject to washing and

vacuum assisted filtration, followed by drying at 45°C for 48 h and stored in a moisture-free environment.

Hybrid silica MSs or matrices: Hybrid MSs were obtained following the same protocol of the inorganic MSs, however the amount and type of silane added to the synthesis was distinct, as shown in Table 1.

Table 1 - Synthesis acronyms and respective silanes' molar percentage

Sample	Silanes in the pre-hydrolyzed solution (mol%)		
	TEOS	MTES	GPTMS
100T	100	0	0
46T:54M	46	54	0
53T:47G	53	0	47
24T:55M:21G	24	55	21

RESULTS & DISCUSSION

Figure 1 shows SEM images, at different magnifications, of the 100T, 46T:54M, 53T:47G and 24T:55M:21G MSs or matrices, exhibiting their differences in terms of morphology, size and porosity. It was observed that the samples containing GPTMS as Si precursor, exhibited lower levels of inner mesoporosity, but consisted of particles with a "worm-like" morphology, possibly due to polymerization-induced (spinodal-type) phase separation, which is accomplished in parallel with the sol-gel transition. This type of morphology might enable the storage of macromolecules in the empty spaces present between the aggregates, acting as a scaffold for chemicals and molecules immobilization. The entrapment of larger molecules, can indeed be carried out on a later stage, after their synthesis, through e.g. soaking under low vacuum conditions. On the other hand, the 100T and 46T:54M MSs consisted of round sphere particles with mesoporosity. The TEOS-MTES derived sample has larger mesopores than the inorganic silica one (100T), which may contribute

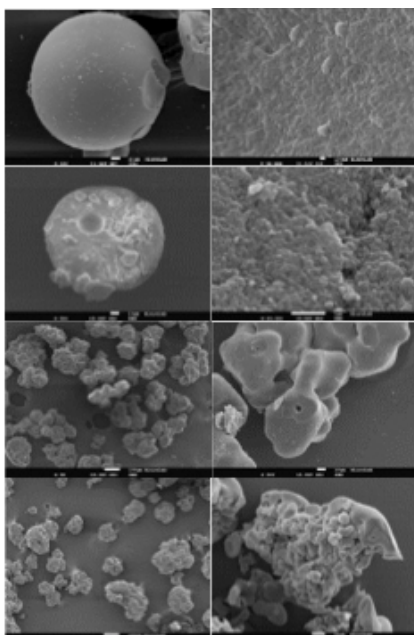


Fig. 1 - SEM images from top to bottom 100T, 46T:54M, 53T:47G and 24T:55M:21G samples with different magnifications

to enclose larger molecules than 100T, during the MSs' synthesis.

So, chemicals and biomolecules may be entrapped not only during the synthesis, in the inner mesoporosity of the developed matrices, or scaffolds (mainly on TEOS and TEOS-MTES derived MSs), but also in a subsequent step, with the aid of a low vacuum system, within the spaces of the worm-like structures, achieved mainly for the TEOS-GPTMS and TEOS-MTES-GPMS derived matrices. It should be stressed that silica-based materials tend to dissolve when soaked in simulated body fluid [3].

From the FTIR results it (Figure 2) was possible to detect the presence of the organic functionalities brought by the Si precursors used in this work in the respective samples, confirming the success of their incorporation in the matrices. The peak at 1030 cm^{-1} and the shoulder at ca. 1200 cm^{-1} , visible in all samples, are both typical of silica-based materials, being correlated to the asymmetric stretching of the siloxane bonds Si-O-Si (TO component) and to the LO component of said asymmetric stretching, respectively. The organic functionality brought by

MTES can be detected by the presence of peaks located at 1270 cm^{-1} and 770 cm^{-1} , ascribed to Si-CH₃ groups, blocks of methyl T units in the organosilicon compound, in samples 46T:54M and 24T:55M:21G. The presence of glycidyloxy groups (from GPTMS) can be detected by the presence of the peaks located at 1250 cm^{-1} and those at 906 cm^{-1} and 850 cm^{-1} , ascribed to C-O and C-O-C stretching of the epoxy (oxirane) groups. Comparing the 53T:47G and 24T:55M:21G matrices it is possible to affirm that both peaks ascribed to epoxy groups are more intense in the 53T:47G MCs spectra, which is in agreement with the higher molar content of GPTMS used in the synthesis of 53T:47G sample.



CONCLUSION

A variety of silica based matrices, in the form of porous microspheres, or in the form of "worm-like" microparticles has been developed by sol-gel processing combined with a microemulsion technique, using different Si precursors (TEOS, MTES and GPTMS) and their combination. It should be noted that the use of such a large molar contents of methyl silane and glycidyloxy silane (MTES and GPTMS) in combination with TEOS, for the preparation of such microparticles, has not yet been described in the state of art. From the FTIR analysis, it was possible to confirm the presence of both methyl and glycidyloxy organic functionalities, brought by the respective silanes and, therefore, confirm the success of the hybrid matrices synthe-

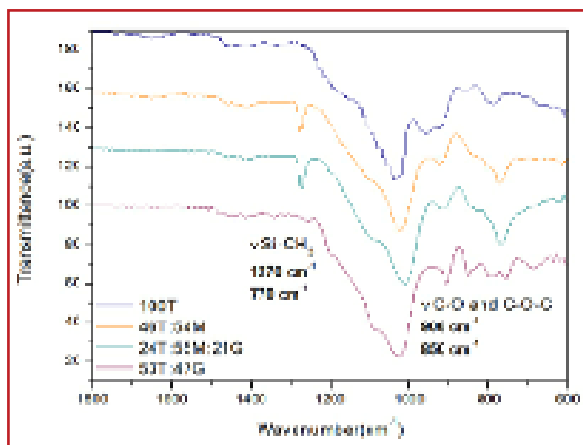


Fig. 2 - FTIR spectra of the inorganic & hybrid samples

sis. The different morphology, porosity and the organic functionality characteristic from the four types of sol-gel derived matrices herein presented enable a customized immobilization or entrapment of a variety of chemical (bio) species of both small and large size molecules, with the 100T and 46T:54M being more appropriate for small molecules and the 53T:47G and 24T:55M:21G more appropriate for larger molecules. Such technology platform is a promising tool for controlled drug delivery. As future development, it would be interesting to study concrete applications of the developed MSs as bio-carriers or as chemical storage for bio-applications. If necessary, a fine-tuning of the synthesis procedure may be carried out to make it more suitable for this type of applications, such as decreasing the processing temperatures.

REFERENCES

1. Kaltzakorta and E. Erkizia, Study on the effect of sol-gel parameters on the size and morphology of silica microcapsules containing different organic compounds. *Phys. Status Solidi*, 7, 2697-2700 (2010).
2. C. J. Barbé, L. Kong, K. S. Finnie, S. Calleja, J. V. Hanna et al., Sol-gel matrices for controlled release: from macro to nano using emulsion polymerisation, *J. Sol-Gel Sci. Technol.*, 46, 393-409 (2008).
3. A. C. Marques, R. M. Almeida, A. Thiema, H. Jain, Sol-gel derived glass scaffold with high pore interconnectivity and enhanced bioactivity, *J. Mater. Res.* 24, 3495-3502 (2009).



Mónica Loureiro
Instituto Superior Tecnico Lisbon
Lisbon - Portugal
monicaloureiro_90@hotmail.com

Acknowledgements

ACM thanks Fundação para a Ciência e a Tecnologia, FCT, through Post-Doc fellowship (SFRH/BPD/96697/2013) and Greenseal Research, Ltd

OXYGENATION STRATEGY TO MAINTAIN ENCAPSULATED PANCREATIC ISLETS IN HYPOXIA

Mouré A., Laugier C., Lesot M., Puraye I., Bosch S., Poncelet D., Bach J.M., Mosser M. – Oniris, France

INTRODUCTION AND OBJECTIVES

Type 1 diabetes mellitus (T1DM) is a serious chronic autoimmune disease in children and young adults leading to the chronic lack of insulin secretion and the daily need of multiple insulin injections. The subcutaneous transplantation of alginate-encapsulated pancreatic islets (bioartificial pancreas) is a promising therapy for the sustained and tight control of glycaemia in type I diabetes. Encapsulation of pancreatic islets provides a material support to improve islets cells survival and prevents them from graft rejection and chronic autoimmune destruction. Transplantation in the subcutaneous space allows for easy graft removal or replacement, and is validated as the site of insulin administration for decades. However, the subcutaneous space is poorly vascularized in contrast with pancreas where islets benefit from a dense network of capillaries providing a high supply of oxygen and nutrients (Carlsson P.O., 1996). Before the neovascularization of the graft surface (requiring 7 to 10 days), pancreatic islets within the bio-artificial pancreas will experiment low oxygen tension due to the distance between cells and host vascular network (Lovett M., 2009). This hypoxia period impairs islets survival and function, and is responsible for bioartificial pancreas graft failure (Barkai U., 2013). Strategies to provide oxygen within the bio-artificial pancreas still need to be developed. Silicone encapsulated calcium peroxide (silicone-CaO₂; Pedraza E., 2012) was



used for long-term oxygen delivery. Nevertheless, this approach does not achieve a physiological oxygen supply correlated to oxygen requirement by islets. Hemocell (Hemarina, Eurobio) is a biological haemoglobin from a marine worm that provides oxygen along a physiological sigmoid diffusion gradient. We have preliminary investigated a new oxygenation strategy associating silicone-CaO₂ and Hemocell for pseudo-islets of MIN6 insulinoma cell line. Here we assess our oxygenation strategy to maintain alginate-encapsulated primary neonate pig islets (NPIs) functionality in a hypoxic environment. NPIs are an interesting alternative to overcome the lack of human pancreas donors and have been shown to have a higher resistance to hypoxia (Emamaullee J.A., 2006).

MATERIALS & METHODS

NPIs isolation

Porcine islets were isolated from pancreas of 5 to 15 days aged Yucatan pigs (INRA PEGASE, Rennes). Experimental plan and design using animals were approved by the French Pays de la Loire Ethic Committee (approval number: 01074.01/02), according to relevant French guidelines. Briefly, pancreases were cut into small pieces of 1 to 2 mm³ using scissors, then digested with 2.5 mg/mL collagenase (Sigma-Aldrich) and gently agitated for 14 to 16 minutes in a shaking water bath at 37 °C. The digest was filtered through nylon screen (500 µm), washed in HBSS buffer supplemented with 0.5 % BSA, and then placed into petri dishes non cell culture treated containing islets culture medium (Ham's F10 (Dutscher) supplemented with 10 mM glucose, 50 mM IBMX, 2 mM L-glutamine, 10 mM nicotinamide, 100 IU/ml penicillin and 100 mg/ml

streptomycin) supplemented with 5 g/L BSA. NPIs were cultured 24 h in normoxia before encapsulation in alginate (Novamatrix) beads.

Alginate encapsulation

Clinical grade low viscosity and high glucuronate sodium alginate (PRO-NOVA UP LVG, Novamatrix) was solubilized in 0.9% NaCl (w/v) at 2.2% (w/v) by gentle stirring overnight at 4°C and sterilized using a 0.2 µm filtration. Alginate beads (3 mm of diameter) were obtained by extrusion through a 23Gx1 needle using a syringe driver, into a 100 mM CaCl₂ gelation bath for 10 minutes. Alginate beads were washed twice in 0.9% NaCl and then in culture media. Once encapsulated, NPIs were cultured in islets culture medium supplemented with 10% porcine serum.



Oxygenation strategies design and evaluation

The oxygen-generating biomaterial was prepared by mixing 25 % (w/v) calcium peroxide (Sigma-Aldrich) in Sylgard® 184 silicone (Sigma-Aldrich). A volume of 100 µL of silicone-CaO₂ was then degassed and reticulated in 48-wells plates during 24 h at 60 °C. The oxygen carrier Hemocell was co-encapsulated with NPIs in alginate hydrogel at 250 µg/mL before reticulation. The oxygenation strategies were assessed on alginate encapsulated NPIs cultured in normoxia (145,7 mmHg) or in a hypoxia chamber (STEMCELL Technologies) filled with a 1 % O₂ gas (10 mmHg) for up to 7 days. Oxygenation strategies benefit was assessed in terms of islet viability, cellular lysis, metabolic activity and insulin secretion ability. Islet viability was assessed using the Live/Dead dye [Calcein AM and Ethidium bromide, Life Technologies]. Cellular lysis within the islets was evaluated by assaying lactate dehydrogenase activity (LDH,

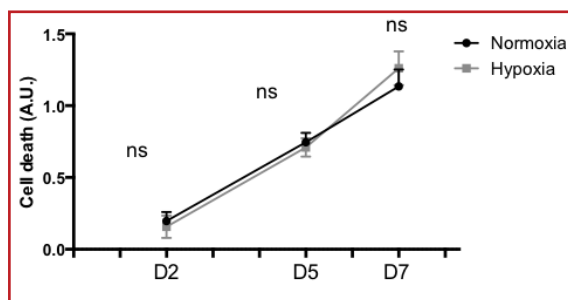


Figure 1: LDH activity in encapsulated NPIs culture supernatant after 2 to 7 days in normoxia or hypoxia

ARTICLE

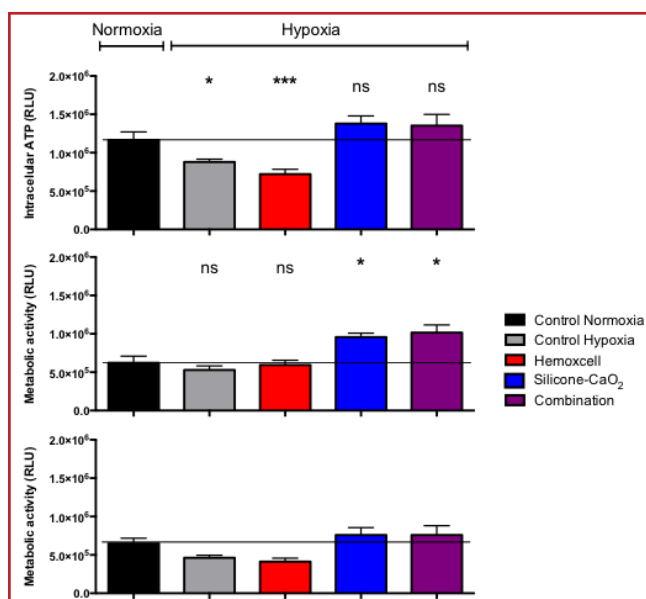


Figure 2: ATP content in encapsulated NPIs after 2, 5 and 7 days of culture in normoxia or hypoxia with or without oxygenation strategies [* p<0.05 ; *** p<0.001]

Roche) in encapsulated NPIs culture supernatants. Metabolic activity of encapsulated NPIs was determined by intracellular ATP content with CellTiter-Glo® 3D Cell Viability kit (Promega). The capacity of encapsulated islets to secrete insulin following a glucose stimulation was evaluated by 30 min sequential incubation of encapsulated islets in basal medium (2.8 mM glucose), stimulation medium (20 mM glucose and 10 mM theophylline) and then again basal medium. Insulin concentrations in each collected samples were assayed by ELISA (Merckodia). The glucose stimulated insulin secretion index was then calculated by dividing the stimulated insulin secretion level by the basal level of the encapsulated islets.

Statistical analysis

Mean differences between groups were assessed by Mann-Whitney test. p<0,05 was considered as significant.

RESULTS & DISCUSSION

NPIs viability

After 2, 5 or 7 days of culture, hypoxia seemed to not significantly affect NPIs viability or LDH activity as compared to normoxia condition (Figure 1).

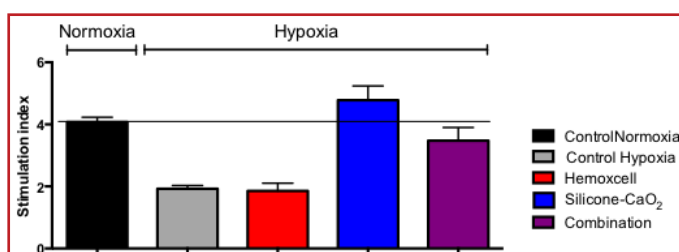


Figure 3: Glucose stimulated insulin secretion index of encapsulated NPIs after 2 days of culture in normoxia or hypoxia with or without oxygenation strategies

Oxygenation strategies toxicity

Silicone-CaO₂ ± Hemoxcell were co-cultured with encapsulated NPIs in normoxia to assess their toxicity. No adverse effect of silicone-CaO₂ nor Hemoxcell was observed on viability, cellular lysis, metabolic activity and insulin secretion.

Oxygenation strategies benefit in hypoxia

Silicone-CaO₂ ± Hemoxcell were co-cultured with encapsulated NPIs in hypoxia. After 2, 5 and 7 days of hypoxia, NPIs ATP content was maintained when culturing with silicone-CaO₂ ± Hemoxcell (Figure 2).

In these conditions, glucose stimulated insulin secretion was maintained similar to normoxia control up to 2 days in the hypoxic environment (Figure 3).

Here we highlighted a natural resistance of encapsulated NPIs to hypoxia in terms of viability, while their metabolic activity and functionality was impaired after 2 day in a hypoxic environment. We confirmed that silicone-CaO₂ supply sufficient oxygen to maintain encapsulated NPIs viability up to 7 days in a hypoxic environment. Furthermore, insulin secretion by porcine islets was maintained up to 2 days in hypoxia. However, no synergic effect of the combination of silicone-CaO₂ and Hemoxcell was observed on encapsulated NPIs.

CONCLUSION

In the pseudo-islet experiment, we highlighted that only the combination of silicone-CaO₂ and Hemoxcell was able to maintain similar pseudo-islet performance compared to normoxia control. While silicone-CaO₂ presented a toxicity in pseudo-islets prevented by Hemoxcell, such toxicity was not evidenced for NPIs. This may be explained by the difference between NPIs and pseudo-islets oxygen consumption rate. This strategy may improve oxygen diffusion to encapsulated islets and decrease oxidative stress thanks to Hemoxcell antioxidant properties. Further oxygen-generating biomaterial and oxygen carrier concentrations need to be investigated in order to improve and extend oxygenation strategy efficiency within the bio-artificial pancreas.

REFERENCES

- Barkai, U. et al. Enhanced oxygen supply improves islet viability in a new bioartificial pancreas. *Cell Transplant.* 22, 1463–1476 (2013).
- Carlsson, P. O. et al. Pancreatic islet blood flow in normal and obese-hyperglycemic (ob/ob) mice. *Am. J. Physiol.* 271, E990–5 (1996).
- Emamaullee, J. A. et al. Neonatal porcine islets exhibit natural resistance to hypoxia-induced apoptosis. *Transplantation* 82, 945–52 (2006).
- Lovett, M. et al. Vascularization strategies for tissue engineering. *Tissue Eng. Part B. Rev.* 15, 353–70 (2009).
- Pedraza, E. et al. Preventing hypoxia-induced cell death in beta cells and islets via hydrolytically activated, oxygen-generating biomaterials. *Proc. Natl. Acad. Sci.* 1–6 (2012).



Anne Moure

Oniris
Nantes, France
anne.moure@oniris-nantes.fr

Acknowledgement

Authors are grateful to Prof J. Miyazaki for the kind gift of the MIN6 cell line

INNOVATIVE NANOCARRIER-BASED TOPICAL FORMULATIONS FOR ALOPECIA TREATMENT

Roque L.*, Dias I., Cruz N., Palma L., Rijo P., and Reis C.; CBIOS, Lisbon, Portugal

INTRODUCTION AND OBJECTIVES

Androgenetic (or pattern) alopecia is a genetically determined disorder characterized by the gradual conversion of terminal hairs into indeterminate, and finally into vellus, hairs. It is an extremely common disease that affects men and women. It generally involves some changes in the protein synthesis of follicular cells such high levels of dihydrotestosterone (DHT) or 5 α -dihydrotestosterone (5 α -DHT). In the human tissues there are two types of 5 α reductases, the type I and the type II. In the hair follicle, the type II is more active in the dermal papillae and the outer sheath of the hair follicle root, which has been described as causes of androgenetic alopecia[1]. Finasteride (FNS) is a 5-alpha reductase type 2 inhibitor. It was firstly described as a synthetic compound for the treatment of benign prostatic hyperplasia and prostate cancer. Lately, it was found that its oral administration may be also useful in the treatment of various dermatological and follicular disorders, particularly, in androgenetic alopecia. However, the oral administration of FNS causes some side effects such as impotence, erectile dysfunction and impairs the reproductive function. Thus, it is necessary to investigate another way to administer the FNS without (or less) adverse side effects. The objectives of this study were to produce and to characterize PLGA NPs with FNS and its inclusion of those NPs in three different formulations (shampoo, lotion and solution).

MATERIAL AND METHODS

All materials were of analytical grade. The preparation of the shampoo consisted in two different phases: the first phase contains a homogeneous mixture of methylparaben, glycerol, sodium lauryl ether sulfate and essence. The second phase contains citric acid buffer in water. The lotion was prepared using Carbopol 940[®],

essence, propylene glycol and isopropyl alcohol. Finally, the solution was made of water, propylene glycol and ethanol.



Preparation of NPs

NPs were prepared through emulsification/ solvent diffusion method in triplicate.

Encapsulation efficiency

The encapsulation efficiency (EE) of FNS was measured in supernatant using a UV-visible spectrophotometry method at 210nm [3]

Particle size analysis

Mean particle size, polydispersity index (PI) and zeta potential of the particles were measured with a Coulter Nanosizer Delsa Nano[™]C (Fullerton, CA, USA).

Morphology

The morphological analysis of the NPs was conducted by using scanning electron microscopy (SEM, CM12 Philips, Netherlands).

In vitro drug release

NPs were placed in 10 mL of PBS (pH 7.4) incubated at 32 °C under constant stirring (130 rpm). At appropriated time intervals, aliquots of the medium were collected and replaced immediately with fresh solution. A clear supernatant was obtained after centrifugation (6300 rpm for 5 min). FNS concentration in the supernatant was determined using previous

method[4]

In vitro permeation tests

After inclusion of the FNS-loaded NPs into the three different formulations, permeation fluxes were accessed using Franz-type static glass diffusion cells with a receptor volume of 4 mL and a diffusion area of 0.95 cm². The receptor phase was PBS at pH=7.4. Synthetic membranes of polydimethylsiloxane were cut to size and then washed with water in order to remove surface contamination. This assay was performed at 32 °C in triplicate. Steady-state fluxes of FNS in each system were determined through the slope of the graph cumulative amount diffused versus time obtained once steady-state diffusion was reached. The permeability coefficient was determined through the ratio of the flux-values and the concentration of the permeant in each vehicle.



Safety test of the excipients using human volunteers

Excipients safety test was performed after in vitro cytotoxicity evaluation.

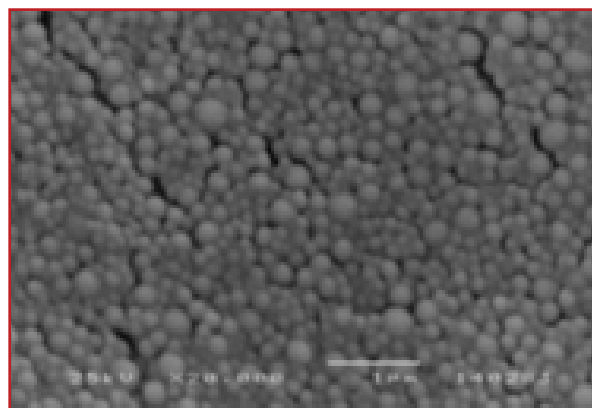


Figure 1 – An example of a SEM image of FNS-loaded NPs (magnification 20000x, scale bar 1 micron).

ARTICLE

Cytotoxicity studies were firstly performed using *S. cerevisiae*. Thereafter, human safety studies were made to evaluate the formulation excipients by the Occluded Patch Test method. Ten volunteers (female, 23 ± 2 years old) were included. Two adhesives were applied to the lower back of each subject over a period of 24 hours. Such adhesives contained 100 μ L of each type of formulation (shampoo, lotion and solution) with empty NPs and without NPs. FNS was not tested in any conditions. Distilled water was the negative control. Primary reactions were visually determined on each volunteer. Transepidermal water loss was measured using a Tewameter TM300 of Courage-Khazaka electronics, after 24 h of contact. The erythema grade was also evaluated using the Chromameter CR400. All the tests were carried out according to the Declaration of Helsinki and received the approval of local Ethical Committee.

RESULTS AND DISCUSSION

NPs were easily prepared by emulsification/ solvent diffusion method. The resultant particle size was $316.5 \text{ nm} \pm 14.44$ (PI 0.114) and 185.3 nm (PI 0.122) for the NPs with FNS and the NPs without the FNS, respectively. This particle size is adequate for drug skin permeation and drug retention in the follicle. Zeta potential was negative with a mean value of $-5.71 \pm 0.43 \text{ mV}$. SEM analysis confirmed the mean particle size and showed that spherical PLGA par-

ticles were easily obtained using standardized and reproducible conditions (Figure 1).

NPs showed an EE value of FNS around $79.49 \pm 0.47\%$. This fact means that the interaction established between the PLGA and the FNS is very probable. Drug release profiles indicated a delayed release of FNS from the particles (Figure 2). It was observed that the percentage of released FNS was about 100% after a period of 3 hours (Figure 2).

Permeation studies revealed that the permeation fluxes of all formulation were very similar until 8h (Figure 3). Thereafter, in the case of the solution, FNS rapidly diffused through the skin.

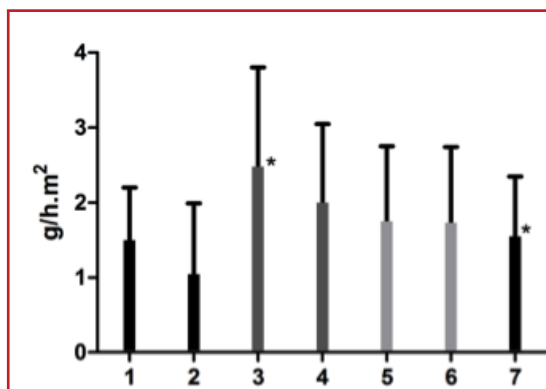


Figure 3 – Transepidermal water loss after 24 h contact of (1) Lotion with NPs, (2) Lotion, (3) Solution with NPs, (4) Solution, (5) Shampoo with NPs, (6) Shampoo, (7) Negative control

No toxic effect of the PLGA NPs was observed in terms of cell viability with *S.cerevisiae* (Figure 4). The same happened with human volunteers where there was a total absence of adverse side effects after 48h contact.

Results of transepidermal water loss demonstrates that 24 hours after the patch application, solution with NPs and shampoo were statistically different from other formulations (Figure 5).

CONCLUSIONS & PERSPECTIVES

Polymeric nanoparticles of FNS have proven to be an efficient encapsulation sys-

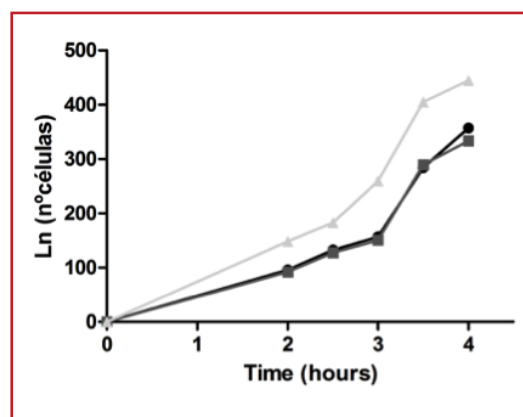


Figure 4– *S. cerevisiae* number of cell over the time

tem, obtaining high values of EE. The permeation tests showed that FNS permeates the skin. Formulation excipients were compatible with the skin. Future studies will include the study of the efficacy and safety of the previous FNS formulations.

REFERENCES

- Libecco, J. F. & Bergfeld, W. F. Finasteride in the treatment of alopecia. Expert Opinion on Pharmacotherapy 5, 933-940 (2004).
- Zhang, H., Cui, W., Bei, J. & Wang, S. Preparation of poly (lactide-co-glycolide-co-caprolactone) nanoparticles and their degradation behaviour in aqueous solution. Polymer degradation and stability 91, 1929-1936 (2006).
- Ulu, S.T. A new spectrophotometric method for the determination of finasteride in tablets. Spectrochimica Acta Part A: Molecular and Biomolecular Spectroscopy 67, 778-783 (2007).
- Reis, C. P., Roque, L. V., Baptista, M. & Rijo, P. Innovative formulation of nystatin particulate systems in toothpaste for candidiasis treatment. Pharm Dev Technol 8, 1-6 (2015).



Luís Roque
University Lusofona
CBIOS
Lisbon - Portugal
luís_roque_10@hotmail.com

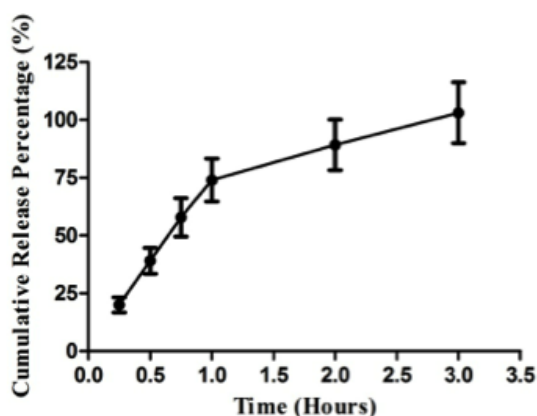


Figure 2– Release of FNS from NPs over the time.

ENHANCING THERMAL STABILITY OF VACCINES USING SILICA

Doekhie, A., Chen, YC., Koumanov, F., van den Elsen, J. and Sartbaeva, A., University of Bath, United Kingdom

INTRODUCTION & OBJECTIVES

Vaccines consist of proteins that, upon administration, will initiate an immune response resulting in prophylactic protection against various pathogens. They are one of the most prominent biologically active compounds that lack thermal stability, resulting in protein denaturation at ambient temperatures. Therefore, vaccines have to be continuously refrigerated during storage and transportation ("cold-chain"). Maintaining specific conditions in cold-chain is frequently problematic, especially in the latter stage of transportation to tropical or developing countries and accounts for a majority of the costs made in general vaccination programs (Galazka et al, 1998). The importance of vaccines in keeping humanity well-protected against various pathogens makes it crucial that we investigate methods to enhance their shelf-life. Our research group has been developing a novel method to protect vaccines from denaturing, thus eliminating the need for continuous refrigeration during storage and transportation. The method is derived from sol-gel technology and involves adding a colloidal suspension of pre-hydrolysed tetraethyl-orthosilicate (TEOS) to proteins in buffer solution. This results in silica particle polymerisation and matrix formation which, in theory, leads to physical entrapment of proteins in their native structure. A recombinant tetanus toxoid C fragment (rTTCF) protein was used as a vaccine model. Our research group has assessed the following objectives to qualify this method suitable for storage and transport of vaccines: 1) silica matrix formation incorporating the TTCF protein. 2) subsequent release of TTCF from silica. 3) analysis of released TTCF from silica to confirm preservation of structural integrity and function.

MATERIALS & METHODS

Purified histidine tagged rTTCF

pET-16b His-tag rTTCF plasmid, developed by Dr A. Knight, was kindly provided by Dr K. Marchbank. Using a heat-shock treatment on a vial of thawed



BL21(DE3) (Novagen, UK), transfection was assessed after an overnight culture on a Luria Broth (LB) agar plate containing ampicillin. Transfected E.coli was cultured in LB medium at 37 °C, 200 rpm. Isopropyl β-D-1-thiogalactopyranoside (IPTG) was used to initiate the 52 kDa TTCF protein production. Bacterial culture was incubated for approx. 5 hours and pellets harvested were stored at -80°C. Using a (Äkta) HisTrap™ column, the rTTCF was bound onto the column followed by gradient elution and collected from pooled fractions to be dialysed against neutral Tris buffer. Pierce™ BCA (Thermo Scientific, UK) analysis was performed to determine yield of purified TTCF in mg/ml.

Silica matrix formation

A solution of pre-hydrolysed TEOS was prepared to be added to TTCF protein in solution. Polymerisation occurred under specific conditions which were time gated. Once the silica matrix formation was completed, the solution was filtered and dry powder was collected after 48 hours at room temperature (RT).

Release of rTTCF from silica

Na-F release buffer was prepared at 190 mM in ddH₂O and acidified with hydrochloric acid (32%). 5 mg of TTCF powder was weighed and added to a 15 ml tube. 5 ml of neutral buffer was added to this tube followed by the addition of 5 ml of release buffer. The tube was placed on a rotator for 1 hour at RT. The released protein was then kept at 4 °C and analysed for structural and functional analysis.

SDS-PAGE

Molecular weight analysis on native and released TTCF sample was carried out by SDS-PAGE gel-

electrophoresis. Samples were run over a 10% linear slab SDS gel using a Mini-Protean3 (Bio-Rad) SDS-PAGE system. Sample and pre-stained ladder (Novex Sharp, Thermo Scientific, UK) were added and the gel was run for 45 min at 200V. Visualisation of sample bands was done using 15-25 ml PageBlue staining overnight at RT.



Western Blot

Confirming histidine residue of native and released TTCF protein was done using Western Blot. SDS-PAGE gel was placed in a semi-dry blotting machine and a current was run at 0.8 mA/cm² to transfer proteins from gel to nitrocellulose membrane, followed by incubation in TBS-Tween with 5 % casein for 35 min at RT. An anti-histidine IgG conjugated with horseradish peroxidase (HRP) antibody was added and incubated for 1 hour at RT. After several washes in TBST, a luminol substrate mixture was added to the membrane followed by luminescent imaging.

UV-Vis

UV-visible absorbance spectra for ana-

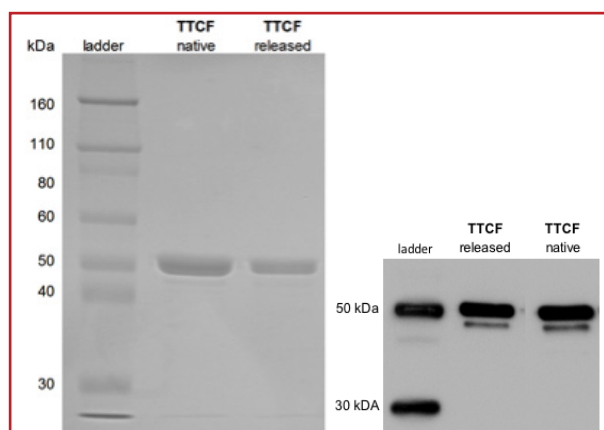


Figure 1. SDS-PAGE and Western Blot of rTTCF. SDS-Page of rTTCF confirms molecular weight (~52 kDa) and release from silica (left) where Western Blot supports this evidence in histidine residue verification (right). No degradation products were observed from released sample.

ARTICLE

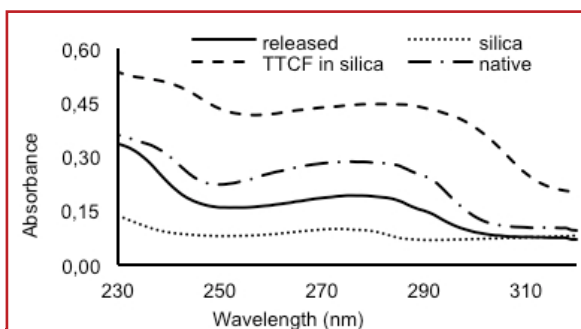


Figure 2. UV-vis of rTTCF aqueous and in silica. UV-vis analysis of rTTCF in native, silica and released forms show peaks at 280 and 230 nm representing protein bonds and tertiary structure UV absorption respectively. Silica in powdered form was used as a control.

lysis of protein absorbance was performed on aqueous samples using a Perkin Elmer Lambda 650 S spectrometer. Range of absorbance analysed was 320–200 nm and samples were prepared to even out protein concentrations and were blanked to their according buffers.

Circular Dichroism

Protein chirality relating to secondary structure in native and released sample was assessed using Far-UV circular dichroism spectrometry. Protein asymmetry was analysed between 185–260 nm using a Chirascan and compared to published data. The [quartz] cuvette path length used was 1 mm. Native and released protein were dialysed against KPO_4 buffer at a neutral pH before measurements.

ELISA

On a 96-wells ELISA plate, rTTCF was bound in 50 mM bicarbonate buffer incubating overnight at 4 °C. The plate was washed with 1x Phosphate Buffered Saline (PBS) and incubated with 1% casein in PBS + Tween20 (0.05 %) for 1 hour at RT followed by repeated washes. A monoclonal antibody against tetanus toxoid, 10G5, was added to each coated well and incubated. Using tetramethylbenzidine (TMB) and 2M sulfuric acid,

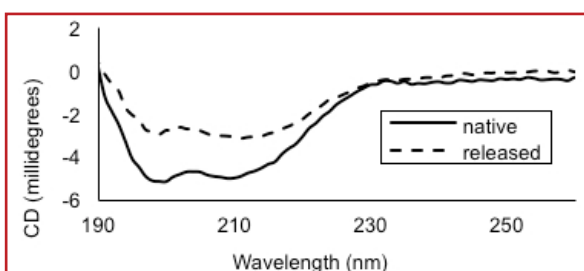


Figure 3. Circular Dichroism of TTCF. CD indicates similar protein asymmetry patterns for both samples.

the reaction was initiated and stopped respectively for OD450nm measurement.

RESULTS AND DISCUSSION

In order to qualify our method as a novel alternative for storing and transporting vaccines at ambient temperatures, we incorporated rTTCF within a silica matrix and stored it at RT prior to analysis. We assessed primary, secondary and tertiary structure of rTTCF, comparing native rTTCF (purified in buffer) to rTTCF released from its protective silica matrix. Primary structure analysis of rTTCF using SDS-page and Western Blot showed that the molecular weight of the protein was unaltered following release from silica (Fig. 1). No additional bands were present which

indicated that there were no degradation products present in the released sample. This is an important result as degradation would reduce the efficacy of any given vaccine. Analysis by UV-vis provided additional evidence of protein preservation as released and native sample present similar absorbance patterns (Fig. 2). Furthermore, UV-vis confirmed successful silica matrix formation around the protein as similar peaks were detected when powder material was analysed. Secondary protein structures, α -helices and β -sheets, were detected using circular dichroism and showed matching reflectivity patterns when comparing native and released (Fig. 3). However, there is a difference in intensity and this could be explained by the presence of minute silica particles left after release, which can interfere with measurements. Alternatively, it might indicate a structural change in protein folding. However, this is unlikely since the ELISA results show equal antibody binding patterns for both released and native rTTCF which suggests the preservation of conformation relating to tertiary protein structure (Fig. 4). From these various analytical tools, it is apparent that our method does not interact or affect structural integrity or function of rTTCF. Immunogeni-

city of rTTCF after release from silica will have to be confirmed by carrying out *in vivo* animal experiments to complete this investigation.

CONCLUSIONS

Our novel methodology provides an exciting opportunity for ambient storage and transport of vaccines. Compared to conventional encapsulation, this method does not need specialised types of synthetic or organic polymers to be developed. rTTCF structure and function seem to be unaffected by our method. Therefore, this could promise an enormous cost-effective solution for other vaccines by reducing energy costs associated with continuous refrigeration. Small angle x-ray scattering experiments are being processed and the results will provide us with greater understanding of the protective capacity of our method. Long-term and thermal stability experiments are ongoing.

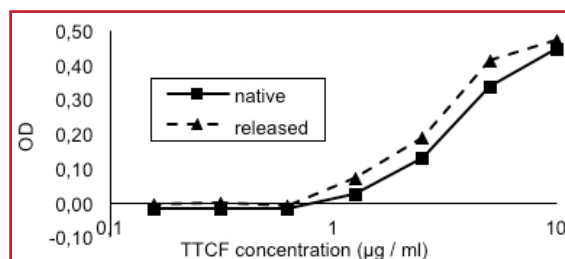


Figure 4. ELISA of rTTCF. ELISA results show similar binding patterns between native and release implying no alteration of antibody binding sites.

REFERENCE

- Galazka A, et al. Thermostability of vaccines. Geneva: World Health Organization; 1998 (WHO/GPV/98.07).



Aswin Doekhie
University of Bath, Chemistry Dept
Bath - UK
ad892@bath.ac.uk

Acknowledgements

Thanks to Dr Kevin Marchbank from Inst. of Cellular Med. at Newcastle Univ. for providing the TTCF plasmid and 10G5 antibody. To Univ. of Bath Alumni Fund & the Annett Trust for providing funding. AS thanks the Royal Society for funding.

CELL-SELECTIVE ENCAPSULATION IN HYDROGEL SHEATHS USING ANTIBODY CONJUGATED HRP

Sengoku, M.¹, Sakai, S.², Taya, M.^{2, 1} Grad. School Frontier Bio.,² Grad. School of Eng. Sci. Osaka University, Japan

INTRODUCTION & OBJECTIVES

Mammalian cell-encapsulation has been studied and advanced since the 1980s for a variety of applications such as cell therapy, fundamental researches in cell biology, and tissue engineering [1-3]. Selective encapsulation of a particular cell fraction from heterogeneous cell populations has potential applications such as studies in cell-to-cell communication, regenerative medicine, and cell therapies. However, there are no versatile methods for realizing this.

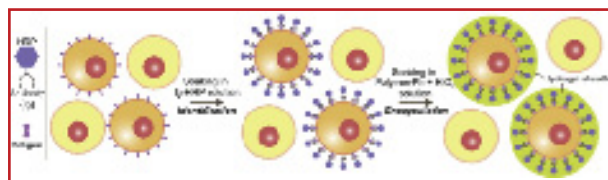


Fig.1 Schematic of cell-selective hydrogel sheath formation on a target cell surface via cell recognition through an antigen-antibody reaction, followed by HRP-catalyzed cross-linking of Ph moieties in polymer molecules.

We first developed the method capable of achieving cell-selective encapsulation which is accomplished through two established technologies: cell recognition via an antigen-antibody reaction and hydrogel formation through a horseradish peroxidase (HRP)-catalyzed reaction. As shown in Fig.1, first, the cells in a particular population are identified from those in heterogeneous populations by antibodies conjugated with HRP. Then, the cells containing both the identified and non-identified ones are soaked in a solution containing H_2O_2 and polymer possessing the moieties crosslinkable through the enzymatic reaction. The hydrogel sheath formation only on the surface of the identified cells is induced by the HRP immobilized with the antibodies.

MATERIAL & METHODS

Floating cell encapsulation

Human hepatoma cell line HepG2 cells were stained with Cell Tracker™ Orange. The cells were mixed with mouse embryo fibroblast-like cell line

10T1/2 cells at 2.5×10^5 cells each, and then soaked in 200 mL DMEM without fetal bovine serum containing IgCD326-HRP at 0.55 mg-antibody/mL for 30 min. The IgCD326-HRP was obtained by conjugating anti-human CD326 antibody from mouse with HRP using commercially available HRP possessing succinimidyl moieties (Peroxidase Labeling kit -NH₂) according to the protocol given by the supplier. After rinsing with phosphate-buffered saline (PBS) twice, the cells were soaked in 200 mL PBS containing 1.0% alginate derivative possessing

Ph and amino fluorescein (AF-Alg-Ph) and 0.1 mM H_2O_2 for 10 min. Derivatives of alginate possessing Ph moieties were synthesized by conjugating sodium alginate with tyramine hydrochloride using 1-ethyl-3-(3-dimethylaminopropyl carbodiimide) and N-hydroxysulfosuccinimide based on previously reported method [4-5]. For evaluating

the cytotoxicity of the encapsulation method, the viability of the cells at each encapsulation step was determined by counting viable cells using a hemocytometer and the trypan-blue exclusion test. In addition, the encapsulated cells prepared from HepG2 cells alone were soaked in the medium containing 0.2 mg/mL alginate lyase for removing the hydrogel sheath and then seeded on a cell culture dish for evaluating the effect of encapsulation on growth of them. Formation of hydrogel sheaths was evaluated using a fluorescence microscope and a flow cytometer after several rinses with PBS.

Adhering cell encapsulation

HepG2 cells stained using Cell Tracker™ Orange and non-stained 10T1/2 cells were seeded in a cell culture dish together. After overnight culture for allowing adhesion of the cells, they were

washed several times using PBS and then soaked in 200 mL PBS containing IgCD326-HRP at 0.55 mg-antibody/mL for 30 min. Subsequently, the cells were rinsed with PBS and then soaked in 100 mL PBS containing 1.0% (w/v) AF-Alg-Ph and 0.1 mM H_2O_2 for 10 min.



Separation of encapsulated cells

HepG2 cells with and without being soaked in IgCD326-HRP solution for 10 min were mixed and then soaked in 1.0% (w/v) AF-Alg-Ph and 0.1 mM H_2O_2 solution for 10 min. The cells soaked in IgCD326-HRP solution were stained with Cell Tracker™ Orange in advance. After rinsing with PBS, the medium containing the cells with and without being encapsulated in AF-Alg-Ph hydrogel sheath were poured on cell culture dish and incubated at 37 °C for 5 h. The content of the HepG2 cells covered by AF-Alg-Ph hydrogel sheath in non-attached cells collected from supernatant medium was measured using a flow cytometer.

RESULTS & DISCUSSION

Possibility of cell-selective encapsulation

As shown in Fig.2a, an AF-Alg-Ph [green] sheath was found only on HepG2

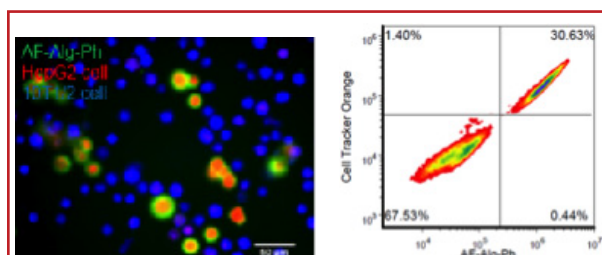


Fig.2 a) The fluorescence image of floating HepG2 cells (red) encapsulated in AF-Alg-Ph (green) and 10T1/2 cells (blue). b) Flowcytometry histograms for Cell Tracker Orange and AF-Alg-Ph obtained for HepG2 cells and 10T1/2 cells after exposure to the cell-selective encapsulation process.

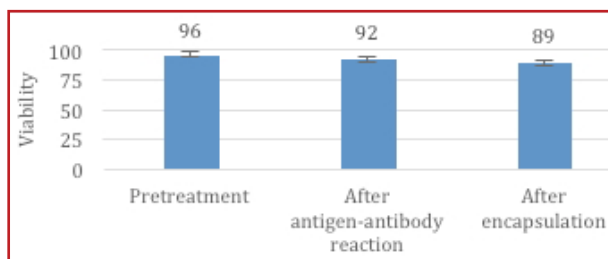


Fig.3 The viability of the cells after antigen-antibody reaction soaking in IgCD326-HRP solution and encapsulation soaking in AF-Alg-Ph and H₂O₂. (n=4)

cells (red) after soaking in a solution containing IgCD326-HRP and a solution containing AF-Alg-Ph and H₂O₂, in sequence. And as shown in Fig.2b, the results of flow cytometry analysis also confirmed hydrogel formation occurred only on HepG2 cells. We confirmed the feasibility of our idea in studies using HepG2 cells expressing CD326 and 10T1/2 cells (blue) not expressing CD326.

As shown in Fig.3, the viability after encapsulation was determined to be 89 %, by the trypan blue exclusion test. This viability result indicates the potential of the cell-selective encapsulation method for subsequent uses of the encapsulated cells. We did not recognize the adverse effects on encapsulated cell viability that could be ascribed to the immobilization of HRP on the cell surface via the antigen-antibody reaction or the subsequent on-cell surface cross-linking by HRP. The viability of around 90% is comparable with values obtained for cells enclosed in hydrogels prepared through whole solution hydrogelation by dissolved HRP and those encapsulated in hydrogel sheaths through HRP immobilization on the cell surface via a non-

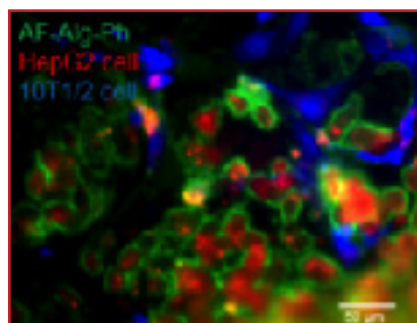


Fig.4 The fluorescence image of adhering HepG2 cells encapsulated in hydrogel sheath and 10T1/2 cells.

cell-selective method. However, H₂O₂ concentration must be carefully chosen in each system because of its well-known cytotoxicity. We chose an H₂O₂ concentration of 0.1 mM, based on the results of preliminary experiments that indicated high viabilities of encapsulated mammalian cells.

Also, we studied the use of adherent cells. As shown in Fig.4, AF-Alg-Ph hydrogel sheaths formed only on adhering HepG2 cells after sequential incubation of the mixture of adhering HepG2 cells and 10T1/2 cells in IgCD326-HRP solution and AF-Alg-Ph and H₂O₂ solution. The cell-selective encapsulation of adhering cells in a hydrogel sheath is expected to be useful for studying cell-cell communication through direct contact.

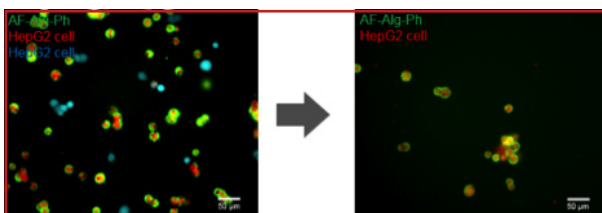


Fig.5 The fluorescence image of a) a mixture of HepG2 cells and 10T1/2 cells in a cell culture dish and b) only HepG2 cells encapsulated in AF-Alg-Ph in supernatant medium removed from cell culture dish.

For potential applications

Additional experiments were carried out from a viewpoint of application of the resultant encapsulated and non-encapsulated cells. In many applications, it would be necessary to separate these cells for subsequent uses. As shown in Fig.5, the encapsulated cells could be separated, in the case where non-encapsulated cells are adherent, simply by plating a mixed suspension of encapsulated and non-encapsulated cells on a cell-adhesion surface. The content of the encapsulated cells in supernatant medium, measured using flow cytometry after 5 h incubation of a suspension containing 27.3% non-encapsulated and 72.0% encapsulated cells, was 96.1%.

CONCLUSIONS & PERSPECTIVES

We first reported the method capable of cell-selective encapsulation in hydrogel sheaths. Cell selectivity was accomplished through an antigen-antibody reaction. Biocompatible encapsulation was accomplished through a cross-linking reaction, catalyzed by an HRP-conjugated antibody immobilized on the cell surface. The cell-selective encapsulation was achieved by the system using an antibody conjugated with HRP. Considering the diversity of available hydrogel sheath materials and commercial antibodies for cell recognition and subsequent hydrogel sheath formation, the method proposed here has huge potential for a wide range of applications, including the creation of novel applications as well as the studies in cell-to-cell communication, regenerative medicine, and cell therapies.

REFERENCES

1. Kang, A., Park, J., et al. Cell encapsulation via microtechnologies. *Biomaterials*. 35, 2651-63 (2014).
2. Huang, X., et al. Microenvironment of alginate-based microcapsules for cell culture and tissue engineering. *J. Biosci. Bioeng.* 114, 1-8 (2012).
3. Chang, TM. Therapeutic applications of polymeric artificial cells. *Nat Rev Drug Discov.* 4, 221-35 (2005).
4. Sakai, S., Kawakami, K. Synthesis and characterization of both ionically and enzymatically crosslinkable alginate. *Acta Biomater.* 3, 495-501 (2007).
5. Sakai, S., Hirose, K., Taguchi, K., et al. An injectable, in situ enzymatically gellable, gelatin derivative for drug delivery and tissue engineering. *Biomaterials*. 30, 3371-7 (2009).



Mikako Sengoku
Osaka Univ.
Frontier Biochemical Science
Toyonaka-city Osaka - Japan
msengo@cheng.es.osaka-u.ac.jp

Acknowledgement

Work supported by Japan Society for the Promotion of Science KAKENHI grant (No. 26630428) from the Ministry of Education, Culture, Sports, Science and Technology of Japan (MEXT).

PRODUCTION OF CARNAUBA WAX PARTICLES FOR COATING IN FLUIDIZED BED

¹Paulo, B., Schmiele, M., Clerici, M., Prata, A. – Unicamp, Brazil – ¹b162410@unicamp.br

INTRODUCTION

Lipid particles are very exploited as they are versatile and can be used both to purposes for improving barrier properties (ie, controlled release and/or permeability), and as active compound. Some lipids are classified as Phase Change Material (PCM) when they have several specific properties, including, high melting enthalpy (Sharma et al., 2009). Carnauba Wax (CW) was investigated in relation to its thermal properties and it was observed that its melting energy is comparable to the classical PCMs (Ribeiro et al., 2013). Its production as particles enables the funcionalization of textiles or building materials as well as the application in solar heating systems. The main techniques used for this purpose are complex coacervation and interfacial polymerization, which result in moist particles, and therefore it's necessary a further drying step. The use of combined techniques, such as the production of particles with a structuration based only on solidification of lipid followed by the subsequent coating in a fluidized bed, may associate high encapsulation efficiency with the required protection to contain the volume variation that occurs during the phase transition. However, there are little knowledge about the use of fluidized bed for coating particles with low melting point (T_m), due to the high susceptibility of the particle to change the phase during the process, hampering its coating. Thus, this step of the project aimed to produce the CW particles using dripping and extrusion techniques, characterize them about their physical and thermal properties, and evaluate their fluid dynamics through the Geldart's classification.

MATERIALS & METHODS

Dripping: the wax was melted at 40 °C above its T_m (78 °C), and dripped ($Q = 6$ mL / min) through a nozzle ($\varnothing = 1$ mm) until a water bath (DRIP_W) or a surfactant solution (1% w/v Tween 80) – (DRIP_T), both at 25 °C situated at 5 cm from the nozzle.

Extrusion: CW powders were added to a double screw extruder ZSK-30 (Wer-



ner and Pfeleiderer, Ramsey, USA), and extruded (screws rotation speed = 150 rpm), under controlled temperature (30, 50, 60 and 60 °C) successively from the supply window to the die, with a hole diameter of 2 (EXT 2) or 4 mm (EXT 4). The product obtained was gently broken into a mill using a sieve opening of 2.8 mm.

All particles obtained were characterized about thermal behavior from 0 °C to 100 °C (2 °C/min) at DSC (2930 Modulated DSC, Ta Instruments, New Castle, Delaware, USA), morphology at stereomicroscope Citoval 2, Carl Zeiss Jena (Berlin, Germany), bulk density, sphericity, roundness. The size analysis was made by sieving for the extruded particles and by image (software ImageJ) for dripped particles.

Low density polyethylene particles (LDPE), which have similar physical properties to CW particles were submitted to fluid dynamic tests in conical-cylindrical fluidized bed (O'hara Technologies, Canada, $D_{max} = 39.7$ cm, $D_{min} = 20$ cm, $H_{conic} = 36$ cm, tilt angle = 55 °) in different amounts (0 to 2500 g) to provide the fluid-dynamic behavior of particles of CW.

RESULTS & DISCUSSION

Table 1. Thermal behavior by Differential Scanning Calorimetry (DSC) obtained for CW particles

Methods	T_m (°C)	ΔH_m (J/g)	T_c (°C)	ΔH_c (J/g)
CW	77.6	198.4	72.3	195.7
EXT 2	78.2	186.9	66.3	184.2
EXT 4	78.3	181.0	72.7	175.9
DRIP_W	77.7	183.7	72.6	178.0
DRIP_T	77.9	156.0	72.1	152.3

Thermal and physical properties, and the adjustment of particles to the Geldart's classification (Geldart, 1973) are presented in Table 1 and 2 and Fig 1, respectively.

From the analysis of the thermal profile, it was observed that T_m e T_c of all particles presented no significant difference when compared to the initial CW. In the general, T_c were 5 °C lower than their T_m , but these values still don't cor-

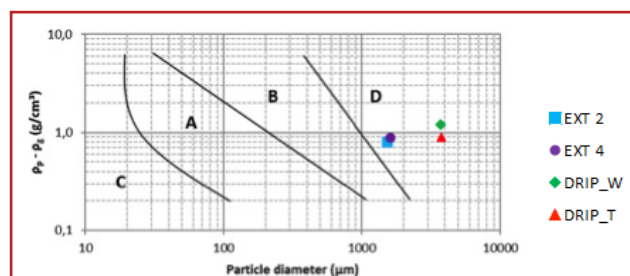


Fig 1. Adjustment of CW particles to Geldart's classification

respond to a sub-cooling process.

In the dripping process, in which was applied high temperatures, particles had a tendency to present lower ΔH_m . Arndt et al. (1984) found that, after subjected to 240 continuous cycles of melting and crystallization, CW showed loss of 15% at constancy of ΔH_m . In a comparative study between the prilling and cold extrusion techniques for the production of particles of saturated fatty acids, Verwaeck et al. (2015) didn't find significant differences in the T_m of the particles produced by different methods, but the particles produced by prilling also showed a lower ΔH_m .

From Table 2, it was observed that lipid particles presented size ranging from 1.5 to 3.8 mm. Note that the particles produced by dripping were significantly larger than those produced by extrusion, due to the intrinsic parameters for each technical influencing the final diameter.

For the dripping system, conditions of flow rate and nozzle diameter determined the particle diameter. A prediction of size based on the Tate's law, indicates that, for

Table 2. Physical properties of CW particles

Physical Properties	Methods of particles production			
	EXT 2	EXT 4	DRIP_W	DRIP_T
Dp (mm)	1.5 ^b ± 0.1	1.6 ^b ± 0.0	3.7 ^a ± 0.6	3.8 ^a ± 0.3
ρ _{bulk} (g/cm ³)	0.5 ^a ± 0.0	0.5 ^b ± 0.0	0.4 ^c ± 0.0	0.4 ^c ± 0.0
ρ _{ap} (g/cm ³)	0.8 ^a ± 0.1	0.9 ^a ± 0.1	1.2 ^a ± 0.4	0.9 ^a ± 0.1
ε	0.326	0.465	0.661	0.520
Roundness	0.7 ^a ± 0.2	0.6 ^b ± 0.1	0.7 ^a ± 0.1	0.8 ^a ± 0.2
Sphericity	0.8 ^a ± 0.1	0.7 ^b ± 0.1	0.7 ^b ± 0.1	0.8 ^a ± 0.2
Figure				

The letters represent a significant difference ($p < 0,05$) in the same line (Tukey's test)

the CW at 120 °C with interfacial tension 32 mN/m and density of 779.94 kg/m³, the particles should have about 3.0 mm, but in addition to the intrinsic properties of the fluid, the operating conditions are critical in particle size. Due to its high melting point and solidification, little changes in temperature over the jacketed line was sufficient to cause clogging and a rise in its viscosity.

In the extrusion process, although the particles were subjected to matrices with different diameters, the milling process interfered significantly in the final particle size, which was carried out under the same conditions for both processes.

The shape of the particles produced by dripping is greatly influenced by the interfacial tension and temperature of the bath where the particle is collected. Table 2 shows that particles produced by dripping have a large variation in their shape. The CW has HLB 12, indicating that it is not extremely hydrophobic and therefore it deforms easier in contact with water. The use of Tween 80 helped to reduce the surface tension between CW and water, and thus it can be seen the significant increasing of the particles sphericity, which is interesting, because spherical particles have a better quality

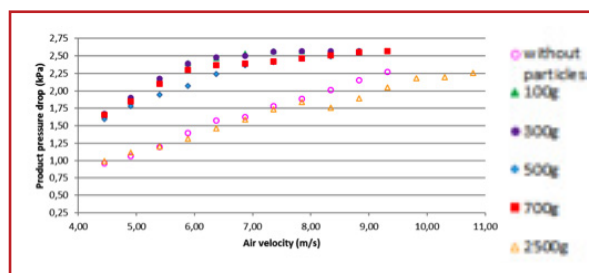


Figure 2. Fluid dynamic tests for LDPE particles

of fluidization (Liu et al., 2008)

The particles produced by dripping presented higher bulk density and lower porosity in relation to the extruded particles, because the increasing of particle size resulted in the increasing of voids in the particle bed.

From the diameter and particle density, it was classified qualitatively the lipid

particles as belonging to group D of Geldart's diagram (Fig. 1). The fluid dynamic tests of the LDPE particles ($D_p = 3000 \mu\text{m}$, $\rho_{ap} = 0.950 \text{ g/cm}^3$) also belonging to the group D, are shown in Fig 2. It was observed that extreme amounts of particles (0 to 2500 g) presented data that are not characteristic of fluidization curve. For amounts of particles between 100 and 700 g, the minimum fluidization velocity is 6.37 m/s, which showed good fluidization in a qualitative way. However, it's suggested to employ intermediate amounts between 300 and 500 g, because low amounts have a tendency to adhere on the wall due to electrostatic energy, while high amounts have a tendency to accommodate in the gas distribution plate and, thus, the fluid dynamic behavior becomes not suitable. In addition, the data don't correspond to the literature, because with the increasing of particle mass, there wasn't increasing of pressure drop, caused, perhaps, by the high porosity of particle bed. In the general, it can say that the fluid dynamic of LDPE particles may predict a good fluidization of wax carnauba particles, which can be coated through this technique.

CONCLUSION & PERSPECTIVES

The cold extrusion and dripping techniques were tested to produce spherical particles of CW to be coated in a fluidized bed. Greater sphericity were obtained for particles produced by extrusion with a 2 mm diameter die, and dripping using surfactant, which was effective



in improving the immersion of the particles in the cooling bath. The particles produced by dripping had a tendency to have lower melting heat, probably due to overheating process. All particles were classified as belonging to Group D, and fluid dynamic tests obtained with LDPE particles may predict a good fluidization of these particles in amounts between 100 and 700 g, in which the minimum fluidization velocity was 6,37 m/s. The extrusion seems more advantageous, especially due to its ability to be a fast and continuous process in a large scale, with easy temperature control and cleanliness, avoiding thermal degradation of CW.

REFERENCES

- Arndt, P. E.; Dunn, J. G.; Willix, R. L. S. Organic compounds as candidate phase change materials in thermal energy storage. *Thermochimica Acta*. 79, 55–68, (1984).
- Geldart, D. Types of Fluidization. *Powder Technol.* 7, 285–292 (1973).
- Liu, B., Zhang, X., Wang, L., Hong, H. Fluidization of non-spherical particles: Sphericity, Zingg factor and other fluidization parameters, *Particology*, 6, 125–129, (2008).
- Sharma, A.; Tyagi, V.V.; Chen, C.R.; Buddhi, D. Review on thermal energy storage with phase change materials and applications. *Renew. Sustainable Energy Rev.* 13, 318–345 (2009).
- Ribeiro, L. F. V.; Silva, V. M.; Soares, A. S. P. Investigation of Phase Change Material Encapsulation by Complex Coacervation. *J. Colloid Sci. Biotechnol.* 2, 78–85 (2013).



Bruna Paulo

Unicamp
Food Engineering
Campinas Sao Paulo - Brazil
brunabarbonpaulo@gmail.com

Acknowledgement

Fapesp (Processes 2011/04230-5 and 2015/11629-2)

EFFECT OF FREE RADICALS PRODUCED BY ENZYME MICROCAPSULES ON CANCER CELLS

Majerská, M., Jakubec, M., Štěpánek, F. - UCT, Czech Rep. Král, V. - UCT & IMG ASCR, v.v.i., Czech Rep.

INTRODUCTION AND OBJECTIVE

In targeted drug delivery systems, a choice of materials for carriers of pharmaceutically active substances to designated tissues plays a very important role. Natural polysaccharides, such as chitosan or alginate, are one of the most promising materials that can be used for this purpose. Chitosan is a linear copolymer consisting of N-acetyl-D-glucosamine and D-glucosamine units. It is formed by deacetylation of chitin, the second most abundant polysaccharide on the Earth. Alginate, isolated from brown algae, is a copolymer composed of β -D-mannuronic and α -L-guluronic acid. Due to properties such as non-toxicity, biocompatibility, biodegradability and bioadhesivity, these polysaccharides are often tested for topical or gastrointestinal drug delivery systems. For example, chitosan is mainly studied for colon drug delivery, because it was found out that chitosan is degraded by microflora present in the colon (Hejazi & Amiji, 2003).



Encapsulation of active substances into suitable carrier systems can not only increase accumulation of these compounds in targeted tissues and minimize their systemic toxic effects, but also protect them in the case of their *in vivo* instability. Sometimes, when it comes to very instable compounds, it is even preferable to encapsulate only their precursors and active compounds will be formed from these precursors in designated places by a chemical reaction.

Laccases (EC 1.10.3.2) belong to a small family of so-called blue copper oxidases, which are mostly found

in higher plants or fungi. These enzymes can oxidise various substrates, such as phenols, aromatic or aliphatic amines. In general, substrate oxidation by laccases is a one-electron reaction generating a free radical with the concomitant reduction of molecular oxygen to water. The pH optima of laccases are highly dependent on substrates. For example, in the case of 2,2'-azino-bis(3-ethylbenzothiazoline-6-sulphonic acid) (ABTS) substrate, a pH optimum is in the range 3-5 (Heinz-kill et al., 1998).



**UNIVERSITY OF
CHEMISTRY AND
TECHNOLOGY
PRAGUE**

ABTS radical belongs to a group of so-called reactive oxygen species (ROS). ROS play a very important role in a cell life. Production of ROS by cells was for the first time observed in phagocytic cells as an immune response to microbial invasion. Since then, it was found out that all cells are capable of ROS generation and that small amounts of ROS are in fact beneficial for cells. For example, increase of H_2O_2 in nanomolar levels in cells is required for cell re-entry to cell cycle (Burch & Heinz, 2005). But in the case of "redox regulation" imbalance, also called "oxidative stress", when levels of ROS are too high for extended period of time, ROS can not only damage cell structures, such as DNA, proteins, lipids or membranes, but even cause cell apoptosis.

As was already mentioned the pH optimum for the conversion of ABTS substrate to ABTS radical by laccase is between 3 and 5. Although, a physiological pH is maintained in the narrow range 7.2-7.4, in which laccases are almost inactive, this fact could represent an advantage for laccase *in vivo* applications. The reason is that unlike in

normal tissues, the pH of the tumour microenvironment varies usually between 6.4 and 7.2 and even values far below 6 were reported (Vaupel et al., 1989). Moreover, some studies indicate that cancer cells are even more sensitive to ROS than cells of a normal tissue. Therefore, the aim of this work is to study the effect of ABTS radical generated by laccase immobilized in alginate-chitosan microparticles on HT-29 colorectal adenocarcinoma cell line.

MATERIALS AND METHODS

Alginate-chitosan microparticles with immobilized enzyme laccase were prepared by spray drying using Buchi Mini Spray Dryer B-290 with a three-fluid nozzle. An outer phase, composed of 0.5 % w/w solution of sodium alginate and laccase was spray dried consequently with an inner phase of 0.125 % w/w solution of low molecular chitosan under following conditions: an inlet temperature 135 °C, an outlet temperature 50 °C, an inner phase flow 3 ml/min and an outer phase flow 3 ml/min. Surface morphology of particles was analysed by Scanning Electron Microscope (SEM) Jeol JC-5700 and particle size distribution was determined by static light scattering method (Horiba Partica LA-950S2). Activity of immobilized laccase was studied by measuring spectrophoto-

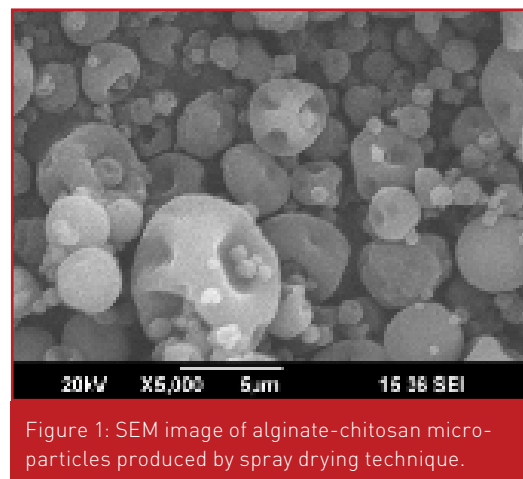


Figure 1: SEM image of alginate-chitosan microparticles produced by spray drying technique.

ARTICLE

metrically the formation of ABTS radical from ABTS substrate at 420 nm.

HT-29 human colon adenocarcinoma cell line (ATCC® HTB-38™) was used for studying cytotoxic effect of ABTS radical on cancer cells. Cells were cultured in DMEM-high glucose medium supplemented with 10 % fetal bovine serum and 1 % antibiotic/antimycotic (A/A) solution in 5 % CO₂ atmosphere and at 37 °C until 70–80 % confluency. As laccase is the most active in the acidic pH, a growth medium, DMEM-high glucose medium supplemented with 1 % A/A, with pH 5.7 was used for cytotoxic tests. The number of viable cells in cytotoxic assays was determined by Cell Counting Kit-8 (Sigma Aldrich), based on the same principle as MTT or MTS test but with higher sensitivity.

RESULTS AND DISCUSSION

Alginate-chitosan microparticles, prepared by spray drying technique, had the mean size of 3.9 μm. They had an irregular shape (Figure 1), which is characteristic of skin-forming materials that undergo a buckling transition once cooled. Although activity of laccase immobilized in the particles was already studied by Kašpar et al. [2013], the experiments were performed only in acetate buffer. In

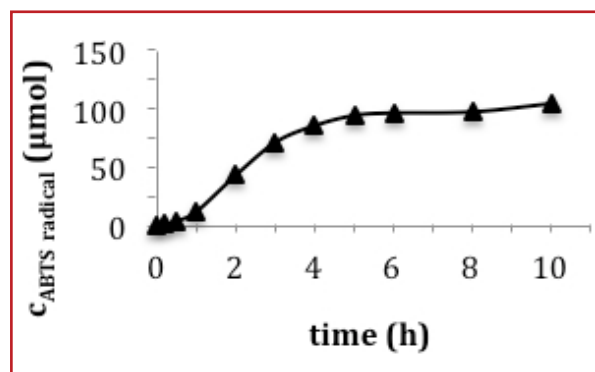


Figure 2: Formation of ABTS radical in time by laccase immobilized in alginate-chitosan microparticles incubated with growth medium (pH 5.7) containing 1 mM ABTS.

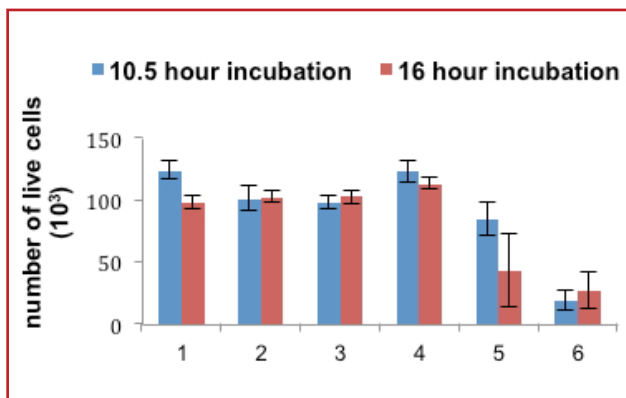


Figure 3: Influence of ABTS radical formation on cell viability. In all samples, cells were incubated in solutions prepared from growth medium (pH 5.7). Samples: growth medium as a control (1), 2.25 μl of free laccase (2), 1 mM ABTS (3), 0.5 mg of microparticles without laccase in 1 mM ABTS (4), 0.5 mg of microparticles with laccase in 1 mM ABTS (5) and 2.25 μl of free laccase in 1 mM ABTS (6).

this study, the activity of the enzyme was also proved in the growth medium (Figure 2). These results are essential for further applications of microparticles to biological systems.

In cytotoxic tests, visible decrease of cell viability was observed only in the samples 5 and 6 where production of ABTS radical took place (Figure 3). In both cases, the formation of ABTS radical was visible by changing of the colour of the solution from yellow (growth medium at pH 5.7) to green (colour of ABTS radical). These results proved the cytotoxic effect of ABTS radical. The fact, that particles without immobilized laccase (sample 4) did not cause decrease of cell viability, makes alginate-chitosan microparticles suitable for application to biological systems.

CONCLUSIONS

It has been shown that prepared alginate-chitosan microparticles containing immobilized laccase are efficient in generating of ABTS radical in physiological solutions at low pH (pH 5.7), characteristic for a tumour microenvironment. Moreover, cytotoxicity of ABTS radical was proved in the case of HT-29 colorectal carcinoma cell line, whereas the toxicity of the particles themselves was not observed. These preliminary re-

sults are promising for the application of the polysaccharide microparticles to biological systems as cancer drug delivery systems. Further studies will focus on the testing of the ABTS radical cytotoxicity on other cancer cell lines. Also microparticle targeting to specific antigens present on the cancer cell surface, such as carbonic anhydrase IX on HT-29 cells, will be studied.

REFERENCES

- Hejazi, R. & Amiji, M. Chitosan-based gastrointestinal delivery systems. *J. Control. Release.* 89, 151-165 (2003).
- Heinzkill, M., Bech, L., Halkier, T. et al. Characterisation of laccases and peroxidases from wood-rotting fungi (family Coprinaceae). *Appl. Environ. Microbiol.* 64, 1601-1606 (1998).
- Burch, P. M. & Hienz, H. H. Redox regulation of cell-cycle re-entry cyclin D1 as a primary target for the mitogenic effects of reactive oxygen and nitrogen species. *Antioxid.Redox Signal.* 7, 741-751 (2005).
- Vaupel, P., Kallinowski, F. & Okunieff, P. Blood flow, oxygen, and nutrient supply, and metabolic microenvironment of human tumors: a review. *Cancer Res.* 49, 6449-6465 (1989).
- Kašpar, O., Tokárová, V., Naynhongo, G. S. et al. Effect of cross-linking method on the activity of spray-dried chitosan microparticles with immobilized laccase. *Food Bioprod. Process.* 91, 525-533 (2013).



Monika Majerska
UCT Prague
Department of Chemical Engineering
Prague - Czech Republic
monika.majerska@vscht.cz

Acknowledgement

We would like to acknowledge support from GA CR 13-37055S and Sotio, a.s.



Journal of Microencapsulation

Vol. 33, Number 3 (2016)

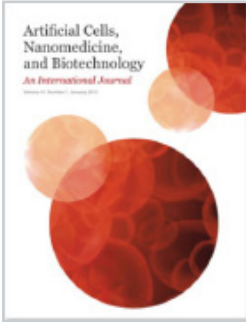
<http://www.tandfonline.com/toc/imnc20/33/3>

- **Polyester-based microparticles of different hydrophobicity: the patterns of lipophilic drug entrapment and release**
Viktor Korzhikov, Ilia Averianov, Evgeniia Litvinchuk & Tatiana B. Tennikova
Pages: 199-208
- **Highly water-soluble mast cell stabiliser-encapsulated solid lipid nanoparticles with enhanced oral bioavailability**
Ravi R. Patel, Sundeep Chaurasia, Gayasuddin Khan, Pramila Chaubey, Nagendra Kumar & Brahmeshwar Mishra
Pages: 209-220
- **Thermal energy storage characteristics of micro-nanoencapsulated heneicosane and octacosane with poly(methylmethacrylate) shell**
Ahmet Sari, Cemil Alkan & Alper Biçer
Pages: 221-228
- **Optimisation of microstructured biodegradable finasteride formulation for depot parenteral application**
Osama A. Ahmed, Amal K. Hussein & Fatma M. Mady
Pages: 229-238
- **In vitro controlled release of clove essential oil in self-assembly of amphiphilic polyethylene glycol-block-polycaprolactone**
O. Thonggoom, N. Punrattanasin, N. Srisawang, N. Promawan & R. Thonggoom
Pages: 239-248
Surfactant-free poly(lactide-co-glycolide) nanoparticles for improving in vitro anticancer efficacy of tetrandrine
- **Polydopamine-coated liposomes as pH-sensitive anticancer drug carriers**
Wei Zong, Ying Hu, Yingchun Su, Nan Luo, Xunan Zhang, Qingchuan Li & Xiaojun Han
Pages: 257-262
- **Tetanus toxoid-loaded cationic non-aggregated nanostructured lipid particles triggered strong humoral and cellular immune responses**
Amandeep Kaur, Kiran Jyoti, Shweta Rai, Rupinder Sidhu, Ravi Shankar Pandey, Upendra Kumar Jain, Anju Katyal & Jitender Madan
Pages: 263-273
- **Concanavaline A conjugated bacterial polyester-based PHBHHx nanoparticles loaded with curcumin for breast cancer therapy**
Ebru Kilicay, Zeynep Karahaliloglu, Baki Hazer, Ishak Özel Tekin & Emir Baki Denkbaz
Pages: 274-285
- **Preparation of high thermal stability polysulfone microcapsules containing lubricant oil and its tribological properties of epoxy composites**
Haiyan Li, Qing Wang, Meiling Li, Yexiang Cui, Yanji Zhu, Baohui Wang & Huaiyuan Wang
Pages: 286-291
- **Metal ion-assisted drug-loading model for novel delivery system of cisplatin solid lipid nanoparticles with improving loading efficiency and sustained release**
Caiqin Yang, Jie Lv, Tao Lv, Yahui Pan, Yazhu Han, Sha Zhao & Jing Wang
Pages: 292-298
- **Formulation of ventlafaxine for once daily administration using polymeric material hybrids**
Howida Kamal Ibrahim & Salwa Salah
Pages: 299-306
- **Preparation of polyurea/melamineformaldehyde double-layered self-healing microcapsules and investigation on core fraction**
Yaoqiang Ming, Jianfeng Hu, Junheng Xing, Minghua Wu & Jinqing Qu
Pages: 307-314
- **Doxorubicin-loaded galactose-conjugated poly(D,L-lactide-co-glycolide) nanoparticles as hepatocyte-targeting drug carrier**
M. Margarida Cardoso, Inês N. Peça, Cláudia D. Raposo, Krasimira T. Petrova, M. Teresa Barros, Rui Gardner & A. Bicho
Pages: 315-322
- **Novel piroxicam-loaded nanospheres generated by the electrospraying technique: physicochemical characterisation and oral bioavailability evaluation**
Omer Mustapha, Fakhar ud Din, Dong Wuk Kim, Jong Hyuck Park, Kyu Bong Woo, Soo-Jeong Lim, Yu Seok Youn, Kwan Hyung Cho, Rehmana Rashid, Abid Mehmood Yousaf, Jong Oh Kim, Chul Soon Yong & Han-Gon Choi
Pages: 323-330
- **Encapsulation methods for photo-polymerisable self-healing formulations**
Wael Ballout, Alain Périchaud, Laura Caserta, Mickael Devassine, Cristina Lavinia Nistor & Rinat Iskakov
Pages: 331-343
- **Separation and nanoencapsulation of antitumor peptides from Chinese three-striped box turtle (Cuora trifasciata)**
Shengjie He, Xinliang Mao, Ting Zhang, Xiaolei Guo, Yazhong Ge, Chungwah Ma & Xuewu Zhang
Pages: 344-354
- **In situ-forming PLGA implants loaded with leuprolide acetate/β-cyclodextrin complexes: mathematical modelling and degradation**
Mehdi Rahimi, Hamid Mobedi & Aliasghar Behnamghader
Pages: 355-364
- **Influence of polyvinylpyrrolidone quantity on the solubility, crystallinity and oral bioavailability of fenofibrate in solvent-evaporated microspheres**
Abid Mehmood Yousaf, Dong Wuk Kim, Dong Shik Kim, Jong Oh Kim, Yu Seok Youn, Kwan Hyung Cho, Chul Soon Yong & Han-Gon Choi
Pages: 365-371
- **Dermal delivery of doxorubicin-loaded solid lipid nanoparticles for the treatment of skin cancer**

Vol. 33, Number 4 (2016)

<http://www.tandfonline.com/toc/imnc20/33/4>

BIBLIOGRAPHY

- Ailar Tupal, Mehdi Sabzichi, Fatemeh Ramezani, Maryam Kouhsoltani & Hamed Hamishehkar
Pages: 372-380
- **Solid lipid nanoparticles carrying lipophilic derivatives of doxorubicin: preparation, characterization, and in vitro cytotoxicity studies**
Elena Peira, Daniela Chirio, Luigi Battaglia, Alessandro Barge, Konstantin Cheghev, Casimiro Luca Gigliotti, Benedetta Ferrara, Chiara Dianzani & Marina Gallarate
Pages: 381-390
 - **Preparation and optimisation of anionic liposomes for delivery of small peptides and cDNA to human corneal epithelial cells**
Luís F. Neves, Jinghua Duan, Adrienne Voelker, Anil Khanal, Lacey McNally, Jill Steinbach-Rankins & Brian P. Ceresa
Pages: 391-399
 - **antimicrobial properties**
Sara Haghju, Sara Beigzadeh, Hadi Almasi & Hamed Hamishehkar
Pages: 438-448
 - **Chitosan films incorporated with nettle (*Urtica Dioica L.*) extract-loaded nanoliposomes: II. Antioxidant activity and release properties**
Hadi Almasi, Mohsen Zandi, Sara Beigzadeh, Sara Haghju & Nazila Mehrnow
Pages: 449-459
 - **Preparation, statistical optimisation and in vitro characterisation of poly (3-hydroxybutyrate-co-3-hydroxyvalerate)/poly (lactic-co-glycolic acid) blend nanoparticles for prolonged delivery of teriparatide**
Nika Bahari Javan, Leila Rezaie Shirmard, Nersi Jafary Omid, Hamid Akbari Javar, Morteza Rafiee Tehrani & Farid Abedin Dorkoosh
Pages: 460-474
 - **Formulation, characterisation and in vivo evaluation of lipid-based nanocarrier for topical delivery of diflunisal**
Amanpreet Kaur, Shishu Goindi & Om Prakash Katara
Pages: 475-486
 - **Alginate-containing systems for oral delivery of superoxide dismutase. Comparison of various configurations and their properties**
Natalia Sudareva, Olga Suvorova, Natalia Saprykina, Alexander Vilesov, Petr Bel'tyukov & Sergey Petunov
Pages: 487-496
 - **cells in regenerative medicine**
Saber Karimineko, Aliakbar Movassaghpour, Amirbahman Rahimzadeh, Mehdi Talebi, Karim Shamsasenan & Abolfazl Akbarzadeh
Pages: 749-757
 - **Pharmaceutical and biomedical applications of quantum dots**
Neha Bajwa, Neelesh K. Mehra, Keerti Jain & Narendra K. Jain
Pages: 758-768
 - **Immunotherapeutic approaches for cancer therapy: An updated review**
Tohid Kazemi, Vahid Younesi, Farhad Jadidi-Niaragh & Mehdi Yousefi
Pages: 769-779
 - **Recent prospective of surface engineered Nanoparticles in the management of Neurodegenerative disorders**
Devendra Singh, Himani Kapahi, Muzamil Rashid, Atish Prakash, Abu Bakar Abdul Majeed & Neeraj Mishra
Pages: 780-791
 - **Preparation of cryogel columns for depletion of hemoglobin from human blood**
Ali Derazshamshir, Gözde Baydemir, Fatma Yılmaz, Nilay Bereli & Adil Denizli
Pages: 792-799
 - **Analysis of the in vitro nanoparticle-cell interactions via a smoothing-splines mixed-effects model**
Elifnur Dogruoz, Savas Dayanik, Gurer Budak & Ihsan Sabuncuoglu
Pages: 800-810
 - **Biogenic silver and gold nanoparticles synthesized using red ginseng root extract, and their applications**
Priyanka Singh, Yeon Ju Kim, Chao Wang, Ramya Mathiyalagan, Mohamed El-Agamy Farh & Deok Chun Yang
Pages: 811-816
 - **pH-sensitive interpenetrating polymer network microspheres of poly(vinyl alcohol) and carboxymethyl cellulose for controlled release of the nonsteroidal anti-inflammatory drug ketorolac tromethamine**
Ebru Kondolot Solak & Akin Er
Pages: 817-824
 - **Capsaicin-loaded vesicular systems designed for enhancing localized delivery for psoriasis therapy**
- Vol. 33, Number 5 (2016)
<http://www.tandfonline.com/toc/imnc20/33/5>
- **Protective effect of magnolol-loaded polyketal microparticles on lipopolysaccharide-induced acute lung injury in rats**
Tsuimin Tsai, Chen-Yu Kao, Chun-Liang Chou, Lu-Chun Liu & Tz-Chong Chou
Pages: 401-411
 - **Production of monodisperse silica gel microspheres for bioencapsulation by extrusion into an oil cross-flow**
Joey J. Benson, Lawrence P. Wackett & Alptekin Aksan
Pages: 412-420
 - **Hollow hydroxyapatite microsphere: a promising carrier for bone tissue engineering**
Hui Yang, Huichang Gao & Yingjun Wang
Pages: 421-426
 - **Preparation and characterisation of the colistin-entrapped liposome driven by electrostatic interaction for intravenous administration**
Yang Li, Lingling Huang, Chengcheng Tang, Enbo Zhang, Lei Ding & Li Yang
Pages: 427-437
 - **Chitosan films incorporated with nettle (*Urtica dioica L.*) extract-loaded nanoliposomes: I. Physicochemical characterisation and**
- 
- Artificial Cells, Nanomedicine and Biotechnology
Vol. 44, Number 3 (2016)
<http://www.tandfonline.com/toc/ianb20/43/5>
- **Implications of mesenchymal stem**

BIBLIOGRAPHY

- Ruchi Gupta, Madhu Gupta, Sharad Mangal, Udit Agrawal & Suresh Prasad Vyas
Pages: 825-834
- **Preparation and characterization of silanized poly(HEMA) nanoparticles for recognition of sugars**
Cansu İlke Kuru, Ceren Türkcan, Murat Uygun, Burcu Okutucu & Sinan Akgöl
Pages: 835-841
 - **Development and evaluation of a sublingual film of the antiemetic granisetron hydrochloride**
Vani Kalia, Tarun Garg, Gautam Rath & Amit Kumar Goyal
Pages: 842-846
 - **Preparation and characterization of gatifloxacin-loaded alginate/poly (vinyl alcohol) electrospun nanofibers**
Saravanakumar Arthanari, Ganesh Mani, Jun Ho Jang, Je O Choi, Yun Ho Cho, Jung Ho Lee, Seung Eun Cha, Han Seok Oh, Deok Han Kwon & Hyun Tae Jang
Pages: 847-852
 - **Useful agents against aflatoxin B1 – antibacterial azomethine and Mn(III) complexes involving L-Threonine, L-Serine, and L-Tyrosine**
Mustafa Anar, Elvan Hasanoğlu Özkan, Hatice Öğütçü, Güleray Açar, İffet Şakıyan & NurŞen Sarı
Pages: 853-858
 - **Research on the bioactivity of isoquercetin extracted from mares-tail on bladder cancer EJ cell and the mechanism of its occurrence**
Juhong Ran, Yanping Wang, Wei Zhang, Minyu Ma & Haiying Zhang
Pages: 859-864
 - **Pharmacological evaluation of nasal delivery of selegiline hydrochloride-loaded thiolated chitosan nanoparticles for the treatment of depression**
Devendra Singh, Muzamil Rashid, Supandeep Singh Hallan, Neelesh Kumar Mehra, Atish Prakash & Neeraj Mishra
Pages: 865-877
 - **Electrospun polycaprolactone matrices with tensile properties suitable for soft tissue engineering**
Anuradha Elamparithi, Alan M. Punnoose, Sarah Kuruville, Mad-daly Ravi, Suresh Rao & Solomon F. D. Paul
Pages: 878-884
 - **Biomedical and biological applications of quantum dots**
Elham Abbasi, Tayebah Kafshdooz, Mohsen Bakhtiary, Nasrin Nikzamir, Nasim Nikzamir, Mohammad Nikzamir, Mozhdeh Mohammadian & Abolfazl Akbarzadeh
Pages: 885-891
 - **Clinical test on circulating tumor cells in peripheral blood of lung cancer patients, based on novel immunomagnetic beads**
Bo Wang, Bin Wang, Daoyun Zhang, Hongyin Guo, Lianbin Zhang & Wen-peng Zhou
Pages: 892-897
 - **In vivo evaluation of novel ketal-based oligosaccharides of hyaluronan micelles as multifunctional CD44 receptor-targeting and tumor pH-responsive carriers**
Daquan Chen, Jingfang Sun, Kaoliang Sun, Wanhui Liu & Zimei Wu
Pages: 898-902
 - **Synthesis and swelling peculiarities of new hydrogels based on the macromolecular reaction of anhydride copolymers with γ -aminopropyltriethoxysilane**
Mahir Timur & Hatice Kaplan Can
Pages: 903-911
 - **Sequence-specific label-free nucleic acid biosensor for the detection of the hepatitis C virus genotype 1a using a disposable pencil graphite electrode**
Soner Donmez, Fatma Arslan & Halit Arslan
Pages: 912-917
 - **Magnetic nanoparticles as potential candidates for biomedical and biological applications**
Fatemeh Zeinali Sehrig, Sima Majidi, Nasrin Nikzamir, Nasim Nikzamir, Mohammad Nikzamir & Abolfazl Akbarzadeh
Pages: 918-927
 - **Diacerein-Loaded novel gastro-retentive nanofiber system using PLLA: Development and in vitro characterization**
Raffi Malik, Tarun Garg, Amit K. Goyal & Goutam Rath
Pages: 928-936
 - **Enhancing the bioavailability of mebendazole by integrating the principles solid dispersion and nanocrystal techniques, for safe and effective management of human echinococcosis**
Sushant Chaudhary, Tarun Garg, Goutam Rath, Rs Rayasa Murthy & Amit K. Goyal
Pages: 937-942
 - **Development of gemcitabine-adsorbed magnetic gelatin nanoparticles for targeted drug delivery in lung cancer**
Senay Hamarat Sanlier, Merve Yasa, Asli Ozge Cihnioglu, Merve Abdulhayoglu, Habibe Yilmaz & Güliz Ak
Pages: 943-949
 - **Preparation of magnetite-chitosan/methylcellulose nanospheres by entrapment and adsorption techniques for targeting the anti-cancer drug 5-fluorouracil**
Oya Şanlı, Asli Kahraman, Ebru Kondolot Solak & Merve Olukman
Pages: 950-959
 - **Formulation, characterization, and evaluation of ligand-conjugated biodegradable quercetin nanoparticles for active targeting**
Anshita Gupta, Chanchal Deep Kaur, Shailendra Saraf & Swarnlata Saraf
Pages: 960-970
 - **An effective electrochemical biosensing platform for the detection of reduced glutathione**
Ülkü Anik, Meliha Çubukçu & F. Nil Ertar
Pages: 971-977
 - **Formulation and optimization of efavirenz nanosuspensions using the precipitation-ultrasonication technique for solubility enhancement**
Sakshi Taneja, Satish Shilpi & Kapil Khatri
Pages: 978-984
 - **Image segmentation and classification of white blood cells with the extreme learning machine and the fast relevance vector machine**
S. Ravikumar
Pages: 985-989
 - **Comparative analysis of cardiovascular effects of selenium nanoparticles and sodium selenite in zebrafish embryos**
Kalimuthu Kalishwaralal, Subhaschandrabose Jeyabharathi, Krishnan Sundar & Azhaguchamy Muthukumar
Pages: 990-996
 - **Inhalable chitosan nanoparticles as antitubercular drug carriers for an effective treatment of tuberculosis**
Tarun Garg, Goutam Rath & Amit K.

BIBLIOGRAPHY

- Goyal
Pages: 997-1001
- **Nano vesicular lipid carriers of angiotensin II receptor blocker: Anti-hypertensive and skin toxicity study in focus**
Abdul Ahad, Mohd. Aqil, Kanchan Kohli, Yasmin Sultana & Mohd. Mujeeb
Pages: 1002-1007
 - **Comparison, synthesis and evaluation of anticancer drug-loaded polymeric nanoparticles on breast cancer cell lines**
Ali Eatemadi, Masoud Darabi, Loghman Afraidooni, Nosratollah Zarghami, Hadis Daraee, Leila Eskandari, Hassan Mellatyar & Abolfazl Akbarzadeh
Pages: 1008-1017
 - **The efficacy of methylene blue encapsulated in silica nanoparticles compared to naked methylene blue for photodynamic applications**
Ghaseb Naser Makhadmeh, Azlan Abdul Aziz & Khairunisak Abdul Razak
Pages: 1018-1022
 - **Ti implants with nanostructured and HA-coated surfaces for improved osseointegration**
Hasret Tolga Sirin, Ibrahim Vargel, Tulin Kutsal, Petek Korkusuz & Erhan Piskin
Pages: 1023-1030
 - **Cisplatin release from dual-responsive magnetic nanocomposites**
Kaveh Kurd, Amir Ahmad Khandagi, Soodabeh Davaran & Abolfazl Akbarzadeh
Pages: 1031-1039
 - **Cartilage-derived extracellular matrix extract promotes chondrocytic phenotype in three-dimensional tissue culture**
Daniel W. Youngstrom, Inese Cakstina & Eriks Jakobsons
Pages: 1040-1047
 - **Evaluation of human cord blood CD34+ hematopoietic stem cell differentiation to megakaryocyte on aminated PES nanofiber scaffold compare to 2-D culture system**
Fatemeh Sabaghi, Karim Shamsasenjan, Ali Akbari Movasaghpour, Naser Amirizadeh, Mahin Nikougofar & Nadia Bagheri
Pages: 1062-1068
 - **Polymerization of modified dapsirin cross-linked hemoglobin (DCLHb) with 1,6-bismaleimic-hexane**
Donglai Qi, Pei Wang, Chen Chen, Song Guo & Xiang Wang
Pages: 1069-1074
 - **Processing of ferulic acid modified hemoglobin**
Song Guo, Pei Wang, Chen Chen, Zhengyan Meng, Donglai Qi & Xiang Wang
Pages: 1075-1079
 - **Bioresorbable polyelectrolytes for smuggling drugs into cells**
Sripriya Jaganathan
Pages: 1080-1097
 - **Ibuprofen microencapsulation within acrylamide-grafted chitosan and methylcellulose interpenetrating polymer network microspheres: Synthesis, characterization, and release studies**
Emine Bulut
Pages: 1098-1108
 - **Silver or gold deposition onto magnetite nanoparticles by using plant extracts as reducing and stabilizing agents**
Araz Norouz Dizaji, Mehmet Yilmaz & Erhan Piskin
Pages: 1109-1115
 - **The effect of silver nanoparticles on zebrafish embryonic development and toxicology**
Guangqing Xia, Tiantian Liu, Zhenwei Wang, Yi Hou, Lihong Dong, Junyi Zhu & Jie Qi
Pages: 1116-1121
 - **Cytocompatibility of PLA/Nano-HA composites for interface fixation**
Weimin Zhu, Daiqi Guo, Yunfang Chen, Weili Xiu, Daping Wang, Jinfang Huang, Jianghong Huang, Wei Lu, Liangquan Peng, Kang Chen & Yanjun Zeng
Pages: 1122-1126
 - **Green synthesis of silver nanoparticles by *Bacillus methylotrophicus*, and their antimicrobial activity**
Chao Wang, Yeon Ju Kim, Priyanka Singh, Ramya Mathiyalagan, Yan Jin & Deok Chun Yang
Pages: 1127-1132
 - **Synthesis of a specific monolithic column with artificial recognition sites for L-glutamic acid via cryo-crosslinking of imprinted nanoparticles**
Ilgim Göktürk, Recep Üzek, Lokman Uzun & Adil Denizli
Pages: 1133-1140
 - **Vascular endothelial growth factor 165-transfected adipose-derived mesenchymal stem cells promote vascularization-assisted fat transplantation**
Chen Jun-jiang & Xi Huan-jiu
Pages: 1141-1149
 - **The development of a green approach for the biosynthesis of silver and gold nanoparticles by using *Panax ginseng* root extract, and their biological applications**
Priyanka Singh, Yeon Ju Kim, Chao Wang, Ramya Mathiyalagan & Deok Chun Yang
Article
 - **Removal of iron by chelation with molecularly imprinted super-macroporous cryogel**
Duygu Çimen, Ilgim Göktürk & Fatma Yılmaz
Pages: 1158-1166
 - **In situ nasal gel drug delivery: A novel approach for brain targeting through the mucosal membrane**
Prabhjot Kaur, Tarun Garg, Goutam Rath & Amit K. Goyal
Pages: 1167-1176
 - **Role of microemulsions in advanced drug delivery**
Aman Kumar Sharma, Tarun Garg, Amit K. Goyal & Goutam Rath
Pages: 1177-1185
 - **Magnetic nanoparticles: Applications in gene delivery and gene therapy**
Sima Majidi, Fatemeh Zeinali Sehrig, Mohammad Samiei, Mor-teza Milani, Elham Abbasi, Kianoosh Dadashzadeh & Abolfazl Akbarzadeh
Pages: 1186-1193
- Vol. 44, Number 4 (2016)
<http://www.tandfonline.com/toc/iab20/44/4>
- **The use of nanoparticles as a promising therapeutic approach in cancer immunotherapy**
Maryam Hosseini, Mostafa Haji-Fatahalaha, Farhad Jadidi-Niaragh, Jafar Majidi & Mehdi Yousefi
Pages: 1051-1061



114 Allée Paul Signac,
44240 Sucé sur Erdre
France
contact@bioencapsulation.net

Bioencapsulation Research Group is a non-profit association promoting networking and research in the encapsulation technology of bioactives. It organises academic conferences and industrial symposiums, publishes newsletters and manages a website.

More information : <http://bioencapsulation.net>

KEEP CONTACT BY REGISTERING ...

Registration is based on a voluntary annual fee. If you wish to simply receive the newsletter and be advised about future events, register online at: <http://bioencapsulation.net>

Be an active member pay the registration fee and get more services

- Reduced registration fees to BRG events
- Full access to conference proceedings (> 1700)
- Access to the forum and internal mailing
- Possibility to contribute to the newsletter
- Reduction for the conference registration
- Priority for awarding of conference grants

Class	Annual fees
Industry members	100 €
Researchers ¹	Free
Students ²	Free
Honorary member and corporate registration ³	1000 €

¹ public and non-profit organizations, contact us for group registration

² registered for a master or PhD program, less than 30 years old.

³ Open access to 1 full page in 1 issues (1/2 page in 2 issues ...) in the newsletter
Registration fees may be paid by credit card, bank transfer or cheque.

For more information or an invoice, see the registration page on <http://bioencapsulation.net>

Thanks to **Agence I** (<http://www.agence-i.eu/>) for designing the newsletter, Brigitte Poncelet (<http://im-pascience.eu>) editing corrections and the editorial board for their help.

STEERING COMMITTEE

- **Prof. Denis Poncelet**, Oniris, France (President)
- **Prof. Stephan Drusch**, TU Berlin, Germany (Secretary)
- **Dr Corinne Hoesli**, McGill University, Canada (Secretary)
- **Prof. Ronald J. Neufeld**, Queen's University, Canada (Treasurer)
- **Prof. Paul De Vos**, Groningen University, Netherlands (Newsletter editor)

- **Dr. Micheal Whelehan**, Solvotrin, Ireland
- **Dr André Brodkorb**, Teagasc Food Research Centre, Ireland (Editor)
- **Dr Thorsten Brandau**, Brace GmbH, Germany [Industrial contact]
- **Prof. Elena Markvicheva**, Institute of Bioorganic Chemistry, Russia
- **Prof Luis Fonseca**, Instituto Superior Técnico, Portugal
- **Prof. Harald Stover**, McMaster University, Canada
- **Dr James Oxley**, SwRI, USA
- **Prof. Igor Lacik**, Polymer Institute, Slovakia
- **Dr Nicole Papen-Botterhuis**, TNO, Netherlands
- **Dr Gabriele Meester**, DSM, Netherlands
- **Dr Amos Nussinovitch**, Hebrew University, Israel
- **Prof Gary Reineccius**, University of Minnesota, USA
- **Dr Laura Hermida**, NITI, Argentina
- **Mr Luis Roque**, Univ. Lusofona, Spain
- **Mrs Catarina Silva**, S Univ. Lusofona, Spain.

REGISTRATION DATA

- Title:
- First name: Last name:
- Affiliation: Department:
- Address: Address (cont.):
- Zipcode: City:
- State: Country:
- Phone: Fax:
- Email: Website:
- Password: Repeat password:
- Registration class: Registration fees: €

Send your registration to : Bioencapsulation Research Group 114 Allée Paul Signac, 44240 Sucé sur Erdre France